

Title Page

Title

Characterization of brain-penetrant pyrimidine-containing molecules with differential microtubule-stabilizing activities developed as potential therapeutic agents for Alzheimer's disease and related tauopathies. €

Authors

Jane Kovalevich, Anne-Sophie Cornec, Yuemang Yao, Michael James, Alexander Crowe, Virginia M-Y Lee, John Q. Trojanowski, Amos B. Smith III, Carlo Ballatore, and Kurt R. Brunden

Primary Laboratory of Origin

Center for Neurodegenerative Disease Research, Institute on Aging, University of Pennsylvania, 3600 Spruce Street, Philadelphia, Pennsylvania 19104-6323 United States

Affiliation

JK, YY, MJ, A-SC, V M-Y L, JQT, CB, KRB; Center for Neurodegenerative Disease Research, Institute on Aging, University of Pennsylvania, 3600 Spruce Street, Philadelphia, Pennsylvania 19104-6323 United States

A-SC, ABS III, CB; Department of Chemistry, School of Arts and Sciences, University of Pennsylvania, 231 South 34th Street, Philadelphia, Pennsylvania 19104-6323, United States

Running Title Page

a) Running Title

Brain-active Microtubule Stabilizers

b) Corresponding Authors

Dr. Kurt R. Brunden, Director of Drug Discovery

Center for Neurodegenerative Disease Research

University of Pennsylvania

3600 Spruce Street – Maloney Building 3rd Floor

Philadelphia, PA 19104-6323

(215) 615-5262

kbrunden@upenn.edu

Dr. Carlo Ballatore

Department of Chemistry

University of Pennsylvania

231 South 34th St.

Philadelphia, PA 19104-6323

bcarlo@sas.upenn.edu

c) Number of text pages: 35 (not including references or figure legends)

Number of tables: 2

Number of figures: 10

Number of references: 52

Number of words in *Abstract*: 250

Number of words in *Introduction*: 750

Number of words in *Discussion*: 1,128

d) Abbreviations

A β – amyloid-beta

AD – Alzheimer's disease

BBB – blood-brain barrier

BCA – bicinchoninic acid

CQ - chloroquine

DAPI - 4',6-diamidino-2-phenylindole

DIV – days in vitro

EDTA – ethylenediaminetetraacetic acid

JPET #231175

EGTA - [ethylenebis(oxyethylenitrilo)]tetraacetic acid

ELISA – enzyme-linked immunosorbent assay

EpoD – epothilone D

FBS – fetal bovine serum

GTP – guanosine triphosphate

HRP – horseradish peroxidase

IACUC – institutional animal care and use committee

i.p. – intraperitoneal

IR – infrared

MES - 4-morpholineethanesulfonic acid

MSB – microtubule stabilization buffer

MT – microtubule

OA – okadaic acid

PBS – phosphate-buffered saline

PDL – poly-D-lysine

Pgp – P-glycoprotein

PI – protease inhibitor

JPET #231175

PIPES - 1,4-piperazinediethanesulfonic acid

PPD – phenylpyrimidine

Ppt – pelletable fraction

PMSF - phenylmethanesulfonyl fluoride

PTM – post-translational modification

RIPA – radioimmunoprecipitation assay

SDS – sodium dodecyl sulfate

SEM – standard error of the mean

Sup – supernatant fraction

TBS – tris-buffered saline

Tg - transgenic

TPD – triazolopyrimidine

Tris - 2-amino-2-hydroxymethylpropane

TSA – trichostatin A

Tub - tubulin

e) Recommended section assignment

Drug Discovery and Translational Medicine

Abstract

The microtubule (MT)-stabilizing protein tau disengages from MTs and forms intracellular inclusions known as neurofibrillary tangles in Alzheimer's disease (AD) and related tauopathies. Reduced tau binding to MTs in tauopathies may contribute to neuronal dysfunction through decreased MT stabilization and disrupted axonal transport. Thus, the introduction of brain-penetrant MT-stabilizing compounds might normalize MT dynamics and axonal deficits in these disorders. We previously described a number of phenylpyrimidines (PPDs) and triazolopyrimidines (TPDs) that induce tubulin post-translational modifications indicative of MT stabilization. We now further characterize the biological properties of these small molecules, and our results reveal that these compounds can be divided into two general classes based on the cellular response they evoke. One group comprised of the PPDs and several TPD examples showed a bell-shaped concentration-response effect on markers of MT stabilization in cellular assays. Moreover, these compounds induced proteasome-dependent degradation of α - and β -tubulin, and caused altered MT morphology in both dividing cells and neuron cultures. In contrast, a second group comprising a subset of TPD molecules (TPD+) increased markers of stable MTs in a concentration-dependent manner in dividing cells and in neurons without affecting total tubulin levels or disrupting MT architecture. Moreover, an example TPD+ compound was shown to increase MTs in a neuron culture model with induced tau hyperphosphorylation and associated MT deficits. Several TPD+ compounds were shown to be both brain-penetrant and orally bioavailable, and a TPD+ example increased MT stabilization in mouse brain, making these compounds potential candidate therapeutics for neurodegenerative tauopathies such as AD.

Introduction

Alzheimer's disease (AD) and related tauopathies are characterized by hyperphosphorylation and aggregation of the microtubule (MT)-associated protein, tau (Lee et al., 2001b; Ballatore et al., 2007). Neuronal tau is normally thought to stabilize MTs and regulate axonal transport, while hyperphosphorylated tau shows reduced interaction with MTs (Alonso et al., 1994; Merrick et al., 1997), facilitating the formation of insoluble tau aggregates termed neurofibrillary tangles and neuropil threads within the neuronal soma and dendritic processes, respectively (Wood et al., 1986; Lee et al., 2001b). Transgenic (tg) mouse models of tauopathy display fewer MTs, increased MT hyperdynamicity, axonal dystrophy and reduced fast axonal transport (FAT) (Zhang et al., 2005; Barten et al., 2012; Zhang et al., 2012). Similarly, there is evidence of MT deficits in AD brain (Hempen and Brion, 1996; Cash et al., 2003). Ultimately, MT abnormalities likely contribute to neuronal dysfunction, neuron loss and cognitive decline, and introduction of MT-stabilizing compounds might attenuate these deficits in AD and related tauopathies (Ballatore et al., 2012; Brunden et al., 2012).

Studies performed in mouse tauopathy models support the hypothesis that increasing MT stability imparts a beneficial effect on neuronal function and disease course. For instance, weekly intraperitoneal (i.p.) injection of the MT-stabilizing compound paclitaxel improved FAT and motor behavior in addition to alleviating spinal cord tau pathology in T44 tau tg mice (Zhang et al., 2005). Although paclitaxel is unable to cross the blood-brain barrier (BBB), sufficient levels of drug likely reached the spinal cord through uptake at neuromuscular junctions (Zhang et al., 2005). More recently, our laboratory has demonstrated that administration of the brain-penetrant MT-stabilizing compound, epothilone D (EpoD), to PS19 tg mice, which develop tau inclusions within the forebrain (Yoshiyama et al., 2007), rescued neuronal loss and attenuated deficits in

axonal architecture, FAT and cognition, while decreasing tau neuropathology (Brunden et al., 2010; Zhang et al., 2012). The salutary effects of EpoD were further confirmed in two additional tau tg mouse models (Barten et al., 2012). Although EpoD has since progressed to clinical trials in AD patients and represents a promising drug candidate, to date it is the only MT-stabilizing agent reported to show beneficial effects in tg mouse models with brain tauopathy. Thus, there is a need to identify alternative brain-penetrant MT-stabilizing agents, ideally those that could be readily synthesized and orally administered.

Cevipabulin (TTI-237), a non-naturally occurring triazolopyrimidine (TPD), has been reported to possess MT-stabilizing activity and efficacy in murine tumor xenograft models (Zhang et al., 2007; Beyer et al., 2008). However, cevipabulin does not cross the BBB and thus would not have therapeutic potential in neurodegenerative disease. We previously reported on the activity of a number of brain-penetrant TPD and phenylpyrimidine (PPD) congeners which possess oral bioavailability and, unlike EpoD, do not inhibit the P-glycoprotein (Pgp) transporter that protects the brain from exposure to xenobiotics and most drugs (Lou et al., 2014; Cornec et al., 2015). In many cases, these compounds demonstrated activity in a QBI-293 cellular assay which measures acetylated tubulin, a post-translational modification (PTM) of the α -tubulin subunit that is thought to occur only on polymerized MTs and is a commonly used marker of stable MTs (Schulze et al., 1987; Brunden et al., 2011; Lou et al., 2014).

Based on potency in the acetyl-tubulin assay and favorable pharmacokinetic properties, the previously disclosed TPD “9” (CNDR-51555) and the PPD “20” (CNDR-51549) (Lou et al., 2014) were chosen for further characterization of biological actions, including evaluation of MT-stabilizing activity in primary neuronal cultures. Notably, these studies revealed several unexpected features in the biological activities of these compounds. In particular, the lead PPD

JPET #231175

and TPD prototypes, as well as many related congeners, revealed unusual bell-shaped or inverse “U” concentration-dependent changes in acetyl-tubulin levels and caused alterations in MT structure. Additionally, these compounds induced degradation of α - and β -tubulin, even at doses that increased acetyl-tubulin levels, and proved ineffective in increasing markers of stable MTs in primary neurons. However, select TPD analogs were identified which retained MT-stabilizing activity without negatively affecting tubulin levels or cytoskeletal architecture. This particular subset of TPDs, hereafter referred to as TPD+ compounds, also promote MT stability in primary neurons and in the cortex of wild-type mice. Furthermore, we demonstrate that TPD+ compounds can rescue MT deficits in neurons treated with okadaic acid (OA), an in vitro model of tau hyperphosphorylation with associated loss of MT structure. Based on their MT-stabilizing activity in cortical neurons and their ability to enter the brain, these TPD+ compounds represent potential therapeutic candidates for the treatment of neurodegenerative tauopathies.

Materials and Methods

Chemistry. EpoD was prepared as previously described (Lee et al., 2001a; Rivkin et al., 2004). The spectroscopic properties of the compound were identical to those reported in the literature. Cevipabulin (CNDR-51533) was synthesized as described (Zhang et al., 2007). All other TPD and PPDs tested were synthesized following published procedures (Zhang et al., 2007; Zhang et al., 2009; Lou et al., 2014) (see Supporting Information). In each case, compound purity was >95% as determined by LC-MS and NMR analyses.

Determination of Plasma and Brain Drug Concentrations. All animal protocols were approved by the University of Pennsylvania Institutional Animal Care and Use Committee (IACUC). Test compounds were administered to CD-1 or B6SJL mice. Both female and male mice were used but were not mixed within experimental groups. The average group age for each study ranged from 2.0 to 5.7 months old. For standard single time-point brain and plasma determinations, mice were injected i.p. with a single dose of 5 mg/kg compound dissolved in DMSO. For oral bioavailability studies, 10 mg/kg compound dissolved in PEG400:dimethylacetamide:water (1:1:1) with 0.5% methyl cellulose was administered via oral gavage. One hour following compound administration, mice were euthanized following an IACUC-approved protocol. Whole brain hemispheres were homogenized in 10 mM ammonium acetate, pH 5.7 (50%, w/v), using a hand-held sonic homogenizer. Plasma was obtained from blood collected in 0.5 M EDTA solution and centrifuged for 10 min at 4,500 x g at 4°C. Fifty µl aliquots of brain homogenate or plasma were mixed with 0.2 ml of acetonitrile, centrifuged at 15,000 x g, and the resultant supernatants were subjected to LC-MS/MS analysis. The LC-MS/MS system includes an Aquity UPLC instrument and a TQ MS instrument controlled using MassLynx software (Waters Corporation, Milford, MA, USA). Compound detection was

performed using multiple reaction monitoring (MRM) of their specific collision-induced ion transitions. Five μ l of each sample was separated on an Aquity BEH C18 column (1.7 μ m, 2.1 mm x 50 mm) at 35°C. Operation was in positive electrospray ionization mode, with mobile phase A of 0.1% (v/v) formic acid and mobile phase B of acetonitrile with 0.1% (v/v) formic acid at a flow rate of 0.6 ml/min using a gradient from 5% to 95% B over 2 min, followed by wash and re-equilibration steps. The MS instrument was operated with a desolvation temperature of 450°C and a source temperature of 150°C. Desolvation and source nitrogen gas flows were 900 and 50 l/h, respectively. Source and MS/MS voltages were optimized for each compound using the MassLynx auto tune utility. Standard curves were generated for each compound from brain homogenate and plasma samples that had compound added at concentrations ranging from 1 to 1,000 nM and extracted as above.

Measurement of Acetyl-Tubulin in Cortical Tissue. Wild-type CD-1 female mice (2-3 months of age) received two injections of 1 or 5 mg/kg CNDR-51657 or -51555 spaced approximately 18 h apart. Four hours following the second injection, mice were euthanized by cardiac perfusion and cortices were dissected from each brain and placed immediately in ice-cold RIPA buffer (50 mM Tris, 150 mM NaCl, 5 mM EDTA, 0.5% sodium deoxycholate, 1% NP-40, 0.1% SDS, pH 8.0) containing protease inhibitor (PI) cocktail (Sigma Aldrich), 1 mM phenylmethylsulfonyl fluoride (PMSF) (Sigma Aldrich), and 3 μ M trichostatin A (TSA) (Sigma Aldrich). Tissue was homogenized with a hand-held battery operated pestle motor mixer and then sonicated to complete the lysis. Samples were centrifuged at 100,000 x g for 30 min at 4°C and supernatant was transferred to a new Eppendorf tube. Remaining pellets were re-suspended in RIPA buffer and homogenized, sonicated, and centrifuged again, as before. Supernatant from the second centrifugation step was pooled with that from first spin. Samples were assessed for protein

concentration by bicinchoninic acid (BCA) assay (Thermo Fisher Scientific) and enzyme-linked immunosorbent assay (ELISA) analysis of acetyl- and alpha-tubulin levels was performed, as described below.

Cell-Free MT Assembly Assay. Compounds CNDR-51555 or -51549 were spotted onto a 384-well clear plate at concentrations derived from serial dilutions starting with 60 μ M to 1.88 μ M. A 0.5 μ L aliquot of each compound was added at 100X the desired final concentration. Ice-cold porcine brain tubulin (30 μ M) (Cytoskeleton Inc, Denver, CO, USA) in PEM buffer (80 mM PIPES, pH 6.8, 5 mM EGTA, 1 mM $MgCl_2$) containing 2 mM GTP was quickly added to each well containing compound. The assembly assay was performed in a SpectraMax M5 plate reader at 37°C with absorbance of 350 nm with reads at 1 min intervals for 45 min. Each assembly reaction was performed in triplicate. At the final time point, material was recovered from wells and samples were centrifuged at 100,000 x g for 30 min at 37°C to sediment assembled tubulin. The supernatants were recovered (“sup” fractions) and pellets (“ppt” fractions) were dissolved in PEM buffer in an equal volume as the sup fraction. For electrophoresis, 5X Laemmli buffer was added to each sup and ppt sample to achieve 1X Laemmli concentration, and samples were boiled at 100°C for 5 min. Two μ L of each sample were loaded per lane on a 10% polyacrylamide gels. Gels were stained with Coomassie blue for quantification of protein in the sup and ppt fractions.

QBI-293, ADR-RES and COS-7 Cell Culture. QBI-293, a derivative of HEK-293, and COS-7 cells (ATCC, Manassas, VA, USA) were maintained in Dulbecco’s Modified Eagle’s Medium (Mediatech Inc, Manassas, VA, USA) containing 10% fetal bovine serum (FBS) (Atlanta Biologicals, Lawrenceville, GA, USA), 2 mM L-glutamine (Mediatech), 50 units/ml penicillin, and 50 μ g/ml streptomycin (1% penicillin/streptomycin; Thermo Fisher Scientific, Waltham,

MA, USA). ADR-RES cells (NCI, Frederick, MD, USA) were maintained in RPMI medium (Mediatech) containing 10% FBS, 2 mM L-glutamine, and 1% penicillin/streptomycin. For compound testing, cells were dissociated with trypsin/EDTA (Thermo Fisher Scientific) and plated at a density of 6×10^5 cells/well in 6-well plates. After overnight incubation, the medium was aspirated and fresh medium containing vehicle or test compound was added. For immunocytochemistry experiments, sterilized glass coverslips coated with 0.1 mg/ml poly-D-lysine (PDL) (Sigma-Aldrich, St. Louis, MO, USA) and 0.1% swine gelatin were placed into 24-well plates. COS-7 cells were plated at a density of 7.5×10^4 cells/well onto the coverslips and incubated overnight prior to compound treatment. Cells were maintained at 37°C in a humidified atmosphere (5% CO₂) for all experiments.

Primary Cortical Neuron Cell Culture. Dissociated primary cortical neurons from embryonic day 18 Sprague Dawley rats were obtained through the University of Pennsylvania tissue culture service. Neurons were plated onto 0.1 mg/ml PDL-coated 6-well plates at a density of 7.5×10^5 cells/well in neurobasal medium (Thermo Fisher Scientific) supplemented with 2% B27 (Thermo Fisher Scientific) and containing 0.5% penicillin/streptomycin. For immunocytochemistry experiments, neurons were plated onto PDL-coated coverslips in 24-well plates at a density of 8.0×10^4 cells/well. Compound treatments were performed at 3, 7 or 10 days in vitro (DIV). For drug treatments, half of the medium was removed from each well and replaced with an equal volume of fresh neuronal medium containing compound (at 2X concentration) to avoid complete medium changes. Neurons were maintained at 37°C in a humidified atmosphere (5% CO₂) for all experiments.

In Vitro Compound Treatment. For experiments requiring proteasomal inhibition, cells were pre-treated with 10 μ M MG-132 (EMD Millipore, Billerica, MA, USA) in DMSO for 2 hours

prior to 4 hour treatment with MT compounds (+/- MG-132). For experiments involving lysosomal inhibition, cells were pre-treated with 100 μ M chloroquine (CQ) for 30 min prior to the addition of MT compounds (+/- CQ). To induce tau hyperphosphorylation in rat primary cortical neurons, 10 DIV cultures were treated for 8 hours with 15 nM okadaic acid (OA). Vinblastine, CQ, and OA were purchased from Sigma-Aldrich and Paclitaxel from Cytoskeleton Inc, while the rest of the MT compounds utilized in this study were synthesized in-house and described in the “Chemistry” section or in Supporting Information.

Pgp Inhibition Assay. ADR-RES cells, which express the human Pgp transporter, were plated at a density of 3.5×10^4 cells/well of 96-well clear plates in 0.1 ml medium. After overnight incubation at 37°C/5% CO₂, cells were treated with 50 μ l verapamil (a Pgp inhibitor; Sigma-Aldrich), cyclosporin A (a Pgp substrate; Sigma-Aldrich) or test compounds dissolved in DMSO and incubated for 17 min (37°C/5% CO₂). Following incubation, 50 μ l of 2 μ M Calcein AM (Thermo Fisher Scientific) was added to each well (final concentration of 1 μ M) and plates were incubated an additional 25 min (37°C/5% CO₂). The medium was removed and cells were washed three times with cold wash buffer [DMEM without phenol red (Thermo Fisher Scientific), 10% FBS, 2 mM L-glutamine]. Calcein fluorescence was analyzed with excitation at 485 nm and emission at 530 nm. Vehicle (0.2% DMSO)-treated cells served as 0% inhibition controls, while 100 μ M verapamil-treated cells served as 100% inhibition controls.

Extraction of Whole-Cell or MT-Enriched Lysates. To obtain whole-cell extract from primary neurons and QBI-293 cells, cells were washed once with 1X phosphate-buffered saline (PBS), (pH 7.4) and then lysed in 200 μ l RIPA buffer containing PI cocktail, 1 mM PMSF, and 1 μ M TSA. Lysed cells were scraped into 1.5 ml Beckman ultracentrifuge tubes (Beckman, Brea, CA, USA), briefly sonicated, and centrifuged at 100,000 x g for 30 min at 4°C. Following

centrifugation, the supernatant from each sample was collected and analyzed for protein content by BCA assay. To separate the free tubulin fraction from the tubulin incorporated into MTs, fractionation under MT-stabilizing conditions was performed. Methods were adapted from a previously reported protocol (Joshi and Cleveland, 1989). Cells were strictly maintained at 37°C and washed with pre-warmed microtubule-stabilization buffer (MSB; 0.1 M MES, 1 mM MgSO₄, 2 mM EGTA, 0.1 mM EDTA, 10% glycerol, pH 6.8). For the extraction of soluble tubulin, 500 µl of MSB containing 1% Triton X-100, 10 µM Paclitaxel (Cytoskeleton Inc.), PI, PMSF and TSA (concentrations same as above) was added to each well and incubated at 37°C for 5 min with occasional gentle agitation. The solution was then transferred to a 1.5 ml Eppendorf tube, and centrifuged for 2 min at 16,000 x g. The supernatant was collected as the soluble (MSB) fraction. Cellular cytoskeletons remaining bound to the tissue culture plate were dissolved in 250 µl (for QBI-293 cells) or 300 µl (for neurons) of SDS buffer (50 mM Tris, 150 mM NaCl, 2% SDS, pH 7.4) plus PI, PMSF and TSA. The cytoskeletal (SDS) fraction was combined with the pellet (if any was obtained) from centrifugation of the Triton-soluble fraction and sonicated to complete the solubilization. The neuronal MSB fraction was concentrated using centrifugal protein concentrators (EMD Millipore) and all samples were brought up to 150 µl (half the volume of the SDS fraction). The protein content in the MSB fraction from QBI cells was sufficient for immunoblotting without performing a concentration step. The MSB fraction was analyzed for protein concentration by BCA assay.

Acetyl- and Alpha-Tubulin ELISA. The ELISA was performed as previously described (Brunden et al., 2011). Briefly, 384-well plates were coated with 12G10 α -tubulin antibody (10 µg/ml; Covance, Princeton, NJ, USA) in 30 µl of cold 0.1 M bicarbonate buffer. 12G10 anti- α -tubulin antibody was originally deposited to the Developmental Studies Hybridoma Bank. After

JPET #231175

overnight incubation at 4°C, the plates were blocked in Block Ace solution (Bio-Rad, Hercules, CA, USA) for a minimum of 24 hours at 4°C. Neuronal or QBI-293 cell homogenates, or cortical homogenates from in vivo studies, were diluted in C buffer (0.02 M sodium phosphate, 2 mM EDTA, 0.4 M NaCl, 1% BSA, 0.005% Thimerosal, pH 7.0). Typically two-fold dilutions from 66.7 ng/μl to 16.7 ng/μl for neurons, 266 ng/μl to 22.2 ng/μl for QBI cells, or 13.3 ng/μl to 6.67 ng/μl for brain homogenate were performed and 30 μl of sample were added to wells in duplicate. Plates were sealed, centrifuged, and incubated overnight at 4°C. Following incubation with antigen, wells were aspirated and washed with PBS containing 0.05% Tween-20 and 0.005% thimerosal (PBS-Tween buffer). A horseradish peroxidase (HRP)-acetyl-tubulin reporter antibody was prepared by conjugating acetyl-tubulin primary antibody (Sigma Aldrich; clone 6-11B-1) to HRP using a commercially available peroxidase labeling kit (Roche Applied Science, Indianapolis, IN, USA). The HRP-acetyl-tubulin reporter antibody (1:1,000 v/v) or pre-conjugated HRP-alpha-tubulin (1:5,000 v/v; ProteinTech Group, Chicago, IL, USA) diluted in C buffer were added to appropriate wells (30 μl per well). The plates were sealed and incubated at room temperature for 4 hours on a platform rocker, followed by washing with PBS-Tween buffer. Peroxidase substrate solution (KPL, Gaithersburg, MD, USA) was added to each well and the reaction was quenched after 10 min with 10% phosphoric acid. Plates were read on a SpectraMax M5 plate reader at an absorbance of 450 nm. The amount of acetyl- and alpha-tubulin protein in each sample was extrapolated using standard curves generated from serial dilutions of known protein standard (acetyl- or alpha-tubulin) concentrations.

Immunoblotting. Equal amounts of protein from cell extracts in RIPA, MSB, or SDS buffers were dissolved in sample buffer, loaded onto 10% polyacrylimide gels (or 15% gels for LC3 detection) and separated by electrophoresis. Protein was then transferred from gels onto 0.2 μm-

pore-size nitrocellulose membranes (Bio-Rad) which were blocked in 5% milk/tris-buffered saline (TBS) for 1 hour at room temperature (23°C). Membranes were then incubated overnight in primary antibody diluted in blocking buffer at 4°C on a rocking platform. Primary antibodies consisted of: acetyl-tubulin (clone 6-11B-1; 1:3,000 v/v; Sigma-Aldrich), 12G10 α -tubulin (1:3,000 v/v; Covance), β -tubulin (1:1,000 v/v; Abcam), de-tyrosinated (glu)-tubulin (1:3,000 v/v; Millipore), ubiquitin (1:1,000 v/v; Millipore), LC3 (1:1,000 v/v; MBL International, Woburn, MA, USA), and AT8 (1:2,000 v/v; Thermo Fisher Scientific). Primary antibodies to GAPDH (1:2,000 v/v; Advanced Immunochemical Inc., Long Beach, CA, USA), beta-actin (1:4,000 v/v; ProteinTech Group), and histone H3 (1:3,000 v/v; Cell Signaling, Danvers, MA, USA) were used as loading controls for quantification. Additionally, a reversible protein staining kit for nitrocellulose membranes (Thermo Fisher Scientific) was utilized to confirm equal protein loading. After overnight incubation in primary antibody, membranes were washed 3 times with TBS containing 0.05% Tween-20 (TBS-T) buffer and then incubated in infrared (IR)-dye-conjugated goat-anti-mouse or goat-anti-rabbit secondary antibodies (1:20,000 v/v; Li-Cor Biosciences, Lincoln, NE, USA) for 1 hour at room temperature. Following incubation with secondary antibodies, membranes were washed 3 times in TBS-T buffer and then imaged using an Odyssey IR imaging system (Li-Cor). Relative protein amounts were quantified using ImageStudio software (Li-Cor) and normalized to loading control proteins.

Immunocytochemistry. Following treatment, primary neurons or COS-7 cells on coverslips were washed rapidly with pre-warmed PEM buffer (80 mM PIPES, 5 mM EGTA, 1 mM MgCl₂, pH 6.8) and fixed with 0.3% glutaraldehyde (in PEM buffer) at 37°C for 10 min. Following fixation, cells were washed and membranes were permeabilized with 0.2% Triton X-100 for 15 min. Unreacted aldehydes were removed by three consecutive 10 minute treatments with 1

mg/ml sodium borohydride diluted in PBS. Coverslips were washed with PBS containing 0.1% Triton X-100 (PBS-T) and incubated in blocking buffer (3% FBS/3% bovine serum albumin in PBS) for 1 hour at room temperature. Acetyl-tubulin (1:3,000 v/v; Sigma Aldrich, St. Louis, MO) and beta-tubulin (1:3,000 v/v; Abcam, Cambridge, MA) antibodies were diluted in blocking buffer and applied overnight at 4°C. After primary antibody incubation, coverslips were washed with PBS-T and incubated with Alexa-fluor-594 or -488-conjugated secondary antibodies (1:2,000 v/v; Thermo Fisher Scientific) for 1 hour at room temperature. After incubation in secondary antibody, coverslips were washed with PBS-T and mounted on double-frosted microscope slides using DAPI fluoromount-G (Southern Biotech, Birmingham, AL, USA) to label nuclei. Slides were imaged by fluorescence microscopy (Olympus, Center Valley, PA, USA) and representative photographs for each condition were acquired.

Statistical Analyses. Linear mixed-effect models were used to compare the outcomes in cell culture studies. The fixed effects in the linear mixed-effects model were the treatment types and replicate runs, whereas experiment-specific random intercepts were used to account for the correlation between repeated measures within an experiment. Treatment effects were assessed with NCSS10 software (Kaysville, UT, USA). Results were plotted graphically and expressed as the average \pm standard error of the mean (SEM) using GraphPad Prism software (La Jolla, CA, USA). Each study that underwent statistical analysis was performed in a minimum of three independent experiments ($n \geq 2$ per study). For in vivo studies, treatment effects were assessed by one-way analysis of variance (ANOVA) with Dunnett's post-hoc test for comparison to vehicle-treated control animals using GraphPad Prism software ($n = 3$ mice per study). P values of < 0.05 were considered statistically significant and indicated as follows: *** $p < 0.001$,

JPET #231175

** $p < 0.01$, and * $p < 0.05$ compared to control. Secondary comparisons between indicated groups were denoted as follows: ††† $p < 0.001$, †† $p < 0.01$, and † $p < 0.05$.

Results

Prototypic PPD and TPD Compounds Induce Proteasome-Dependent Degradation of α -

and β -Tubulin. We previously demonstrated that the prototype PPD and TPD examples CNDR-51549 and CNDR-51555 [compounds 20 and 9, respectively, in (Lou et al., 2014)] (refer to Table 2 for chemical structures) increase levels of acetylated tubulin following 4 hours of treatment with doses up to 1 μ M in QBI-293 cells (Lou et al., 2014). However, further evaluation of these compounds revealed that increasing concentrations beyond 1 μ M no longer increased acetyl-tubulin levels in the QBI-293 cells, as determined by ELISA (Fig. 1A). Thus, rather than observing an additional increase or a plateau effect on acetyl-tubulin levels when tested at 10 μ M, a bell-shaped or inverse “U” concentration-response curve was observed in which both compounds appeared inactive at the highest dose (Fig. 1A). This unusual concentration-response was not observed in assays in which CNDR-51549 or -51555 were incubated with purified tubulin, as a linear concentration-dependent increase was observed both in light-scattering that resulted from the formation of higher order structures, and in the amount of assembled tubulin that was found in the pellet fraction following centrifugation (Supplemental Fig. 1). The observed decrease in acetyl-tubulin in the cellular assay could have resulted from an effect that left stable MTs intact but somehow altered tubulin acetylation. However, immunoblot analysis of deetyrosinated (glu)-tubulin, an independent marker of stable MTs that depends on the enzymatic removal of the COOH-terminus of α -tubulin (Kreis, 1987), revealed that treatment of QBI-293 cells with 1 μ M CNDR-51555 resulted in a significant increase of glu-tubulin, whereas 10 μ M treatment with CNDR-51555 did not increase this marker of stable MTs (Fig. 1, C and D). Interestingly, the 10 μ M treatment with CNDR-51549, which did not increase acetyl-tubulin levels appreciably relative to control cells, still increased glu-tubulin levels above baseline, albeit

to a lesser extent than the 1 μ M concentration of this compound (Fig. 1, E and F). To further investigate the relative absence of effect on stable MT markers following treatment with 10 μ M of the prototypic PPD and TPD compounds, the total amount of cellular α -tubulin available to be incorporated into MTs at each treatment concentration was assessed by ELISA (Fig. 1B). Surprisingly, α -tubulin levels were significantly decreased at concentrations of CNDR-51555 (100 nM and 1 μ M) and CNDR-51549 (1 μ M) that increased acetyl-tubulin and glu-tubulin (Fig. 1, A and C-F). Cellular α -tubulin levels declined in a concentration-dependent manner, with only 27% and 55% of control levels remaining after 4 hours of treatment with 10 μ M CNDR-51555 or CNDR-51549, respectively, as determined by ELISA (Fig. 1B). In accordance with these findings, QBI-293 cells treated with 100 nM of the TPD, cevipabulin (CNDR-51533), also demonstrated a similar decrease in α -tubulin levels (56 \pm 2.7% of those from untreated cells; graph not shown). Assessment of modified (acetyl- and glu-) and total α - and β -tubulin by immunoblot analyses verified the ELISA results, and confirmed that β -tubulin levels are reduced in a similar manner to α -tubulin following treatment with CNDR-51555 (Fig. 1, C and D) or -51549 (Fig. 1, E and F). This effect appeared specific to tubulin, as levels of other cytoskeleton-associated proteins, including beta-actin, were not altered by treatment with either compound.

The observation of decreased α - and β -tubulin levels upon treatment with the PPD and TPD compounds at concentrations that increased acetyl- and glu-tubulin levels was unexpected, particularly given our prior observation that 100 nM cevipabulin treatment appeared to yield normal MT morphology as judged by acetyl-tubulin immunofluorescence staining of QBI-293 cells (Lou et al., 2014). To evaluate morphological changes in the MT network following treatment with the MT-targeted compounds, immunocytochemistry was performed in COS-7 cells, as it is easier to visualize MTs in these cells than in QBI-293 cells. Cells were treated with

vehicle (DMSO), 100 nM EpoD, a natural product believed to bind to the same site on the β -tubulin subunit of assembled MTs as taxol or 1 or 10 μ M CNDR-51555 or -51549. After 4 hours of treatment, the cells were fixed and double-labeled for acetyl-tubulin and β -tubulin. There was a marked increase in acetyl-tubulin immunoreactivity following treatment with EpoD, 1 μ M CNDR-51555 (Fig. 2A) or 1 μ M CNDR-51549 (Supplemental Fig. 2A). However, whereas β -tubulin labeling appeared normal in the EpoD-treated cells, the cells exposed to 1 μ M CNDR-51555 showed some evidence of altered β -tubulin distribution and intensity, and 10 μ M treatment with either CNDR-51555 or CNDR-51549 resulted in barely detectable acetyl-tubulin, with β -tubulin labeling that was diffuse and in the case of CNDR-51555, greatly diminished compared to both control and EpoD-treated cells (Fig. 2 and Supplemental Fig. 2).

There is some precedent for MT-directed agents altering cellular α - and β -tubulin levels, with isothiocyanates having been previously identified as MT-binding compounds capable of inducing rapid tubulin degradation (Mi et al., 2009a). It was suggested that isothiocyanates induce MT-misfolding upon covalent binding to tubulin, with eventual degradation of α - and β -tubulin by an incompletely characterized proteasome-mediated pathway (Mi et al., 2009b). Additionally, another study demonstrated loss of α -tubulin following administration of the vinca alkaloid, vincristine (Huff et al., 2010). However, this effect was only observed in neural HCN2 cells and not in a variety of other cell lines (Huff et al., 2010). In this regard, treatment of QBI-293 cells with 1 μ M of the vinca alkaloid vinblastine, which promotes MT depolymerization and redistribution of tubulin from cytoskeletal to soluble cellular pools (Supplemental Fig. 3, A and B), does not significantly alter total levels of α - or β -tubulin (Supplemental Fig. 3, C, D and E). These findings are significant in light of previous studies which demonstrated that cevipabulin displaced vinblastine in competitive binding assays (Beyer et al., 2008; Beyer et al., 2009). Thus,

if the cevipabulin analog CNDR-51555 interacts with the vinca site of MTs, it elicits an effect on cellular tubulin levels that differs from that of vinblastine.

To elucidate the mechanism of decreased α - and β -tubulin after TPD or PPD treatment, we assessed the contributions of autophagic-lysosomal and proteasomal protein degradation pathways. Autophagic clearance through lysosomal pathways comprises a major mechanism of cellular protein degradation (Mizushima and Komatsu, 2011); we thus treated QBI-293 cells with the lysosome inhibitor, chloroquine (CQ) (Wibo and Poole, 1974), 30 minutes prior to and during administration of 1 μ M CNDR-51555 or -51549 to determine if autophagic inhibition prevented the reduction in tubulin levels. Chloroquine had no effect on the reduction in α -tubulin levels induced by treatment with 1 μ M CNDR-51555 or -51549, as assessed by ELISA (Fig. 3A). Likewise, immunoblot analysis of lysates from QBI-293 cells treated with 1 μ M CNDR-51555 or -51549 in the absence or presence of CQ demonstrated that the compound-mediated decrease in β -tubulin levels could not be rescued by treatment with CQ (Fig. 3, B and C). Accumulation of LC3-II protein (lower molecular weight band on LC3 blot) confirmed effective inhibition of the autophagic pathway in response to CQ (Fig. 3, B and C). Thus, alterations in tubulin levels in response to the prototype TPD and PPD compounds are unlikely due to autophagic protein clearance.

Proteasome-dependent protein degradation represents a highly utilized pathway for cells to degrade unnecessary or damaged proteins (Lecker et al., 2006), and as noted, binding of certain isothiocyanates to MTs has been demonstrated to induce tubulin degradation by proteasomes (Mi et al., 2009a). In this context, 2 hour pre-treatment of QBI-293 cells with the proteasome inhibitor, MG-132, followed by addition of CNDR -51555 for an additional 4 hours, significantly attenuated the loss of α -tubulin observed following treatment with CNDR-51555

alone, as assessed by ELISA analysis of RIPA-soluble cell lysates (Fig. 4A). However, MG-132 only partially rescued tubulin levels in this fraction following treatment with CNDR-51555, and did not rescue α -tubulin loss from the RIPA-soluble fraction of CNDR-51549-treated cells (Fig. 4A). Western blotting of lysates from MG-132-treated cells revealed the presence of accumulated ubiquitinated proteins, thereby confirming proteasome inhibition (Fig. 4B). As proteasome inhibition might lead to the accumulation of ubiquitinated and aggregated proteins with decreased RIPA-solubility (Demasi and Davies, 2003), as has been previously observed for tubulin after treatment of cells with certain isothiocyanates (Mi et al., 2009a; Mi et al., 2009b), the RIPA-insoluble fraction from treated cells was dissolved in 2% SDS-containing buffer and analyzed for tubulin content by immunoblotting. Significant accumulation of α - and β -tubulin was observed in the SDS-soluble fraction from cells treated with the combination of MG-132 and CNDR-51555 or -51549, but not under any other condition (Fig. 4, C and D). As the SDS concentration in the insoluble fraction prevented ELISA analysis, equal proportions of RIPA-soluble and SDS-soluble cellular fractions were combined for each treatment and assessed by immunoblotting, which revealed nearly complete rescue of total α - and β -tubulin levels following dual treatment of MG-132 and CNDR-51555/-51549 compared to compound treatment alone (Fig. 4, E-H). These findings suggest that both of these compounds induce proteasome-dependent tubulin degradation. However, unlike what was previously reported for isothiocyanate-treated cells (Mi et al., 2009a), we observed no evidence of increased insolubility of tubulin in the absence of MG-132, and thus the mechanism by which the PPD and TPD compounds induce tubulin degradation is presently unknown although it may relate to alterations in tubulin conformation.

Identification of a TPD Series that Exhibits MT-Stabilizing Activity without Reducing

Total Tubulin Levels. While our prototypic PPD and TPD compounds appear to possess MT-stabilizing properties at certain concentrations based on increases in acetyl-tubulin and glutubulin, their substantial negative impact on total tubulin levels and apparent disruption of MT architecture likely preclude them from providing any therapeutic benefit in AD or related tauopathies. However, further evaluation of additional members of the TPDs and PPDs (Lou et al., 2014) led to the identification of one compound [CNDR-51597; compound 8 in (Lou et al., 2014)], which induced elevated acetyl-tubulin at concentrations up to 10 μ M without decreasing α -tubulin levels (Table 1 and Fig. 5A). Like CNDR-51555, this compound belongs to the TPD class of heterocycles. However, unlike the former, CNDR-51597 lacks the alkoxy side-chain, suggesting the possibility of a structure-activity relationship in which the nature of the substituent in the para position may be ultimately involved in determining the cellular phenotype. Indeed, among all TPDs tested, those containing an alkoxy side-chain (e.g., cevipabulin, CNDR-51555, and -51567) demonstrated a bell-shaped dose-response curve in the acetyl-tubulin assay, as well as a decrease in total α -tubulin levels (Table 2), whereas TPD congeners in which the side-chain is replaced by a fluoride (e.g., CNDR-51539, -51597, -51647, -51655, and -51657) were found to produce linear dose-responses in the cell-based assays, with no evidence of a reduction of total tubulin (Table 1). Hereafter, we refer to the improved examples in Table 1 as TPD+ compounds. While these results indicate a SAR for the TPD series, all of the PPD compounds elicited a similar cellular phenotype as CNDR-51549 (Table 2), regardless of whether the substituent in the para position is a fluoride or an alkoxy side-chain.

While no TPD+ compounds were active at concentrations of 10 or 100 nM, compounds which increased acetyl-tubulin at 1 μ M underwent additional in vivo testing for brain exposure.

JPET #231175

Wild-type mice received a 5 mg/kg i.p. injection of compound and brain and plasma drug levels were determined one hour post-injection. Resultant average brain levels and blood/plasma (B/P) ratios are indicated in Table 1 for selected compounds. One of the most potent compounds identified in the acetyl-tubulin assay, CNDR-51657, also demonstrated a favorable in vivo profile, with brain levels averaging 812 ± 61 nM and a high B/P ratio of 2.7 ± 0.7 (Table 1). Although previously reported i.p. dosing with CNDR-51555 and -51549 resulted in higher overall brain exposure than CNDR-51657 (1300 nM +/- 200 for CNDR-51555; 2900 nM +/- 100 for CNDR-51549), the B/P ratios were much less favorable (0.27 ± 0.2 for CNDR-51555; 0.58 ± 0.01 for CNDR-51549), thus resulting in much higher peripheral drug exposure (Lou et al., 2014). An average concentration of 670 ± 580 nM of CNDR-51657 was detected in brain tissue of mice one hour after a single oral gavage dosing of 10 mg/kg, revealing that the compound has reasonably good oral absorption in addition to excellent brain exposure.

Finally, the effects of newly synthesized compounds were evaluated for activity in a Pgp inhibition assay. Of the compounds described in Tables 1 and 2, the PPD compound CNDR-51554 and TPD+ compound CNDR-51647 exhibited the highest Pgp inhibitory activity in the assay, achieving 29% and 37% inhibition, respectively, at the highest concentration tested of 33.3 μ M (Supplemental Table 1). CNDR-51657 inhibited Pgp activity by approximately 19% at the 33.3 μ M concentration, but activity decreased in a concentration-dependent manner and was negligible at doses that resulted in increased acetyl-tubulin (Supplemental Fig. 4 and Supplemental Table 1). Full dose-response curves of CNDR-51657 and previously tested compounds EpoD, CNDR-51555, and -51549 are provided (Supplemental Fig. 4). These data suggest the majority of newly synthesized TPD+ compounds would interfere minimally with Pgp function at concentrations that increase acetyl-tubulin.

To characterize the biological actions of the TPD+ compounds in greater depth, CNDR-51657 was selected as a prototype to represent this series and to undergo additional testing for comparison to the original TPD lead, CNDR-51555. CNDR-51657 significantly increased levels of acetylated tubulin at 1 μ M and 10 μ M by 2.4- and 3.9-fold, respectively, as determined by ELISA (Table 1 and Fig. 5B), whereas α -tubulin levels were not decreased at any dose (Fig. 5B). Immunoblot results confirmed that CNDR-51657 also increased levels of glu-tubulin in a dose-dependent manner and did not negatively affect levels of β -tubulin (Fig. 5, C and D). To rule out the possibility that a bell-shaped concentration response in acetyl-tubulin levels or a loss of α -tubulin were not observed with CNDR-51657 simply due to decreased potency of this compound compared to the PPD and TPD prototypes, QBI-293 cells were treated with higher concentrations (10, 30, or 60 μ M) and assessed for levels of acetyl- and α -tubulin by ELISA. A concentration-dependent increase of acetyl-tubulin was observed at these higher compound exposures, and α -tubulin levels remained at those of vehicle-treated cells (Supplemental Fig. 5). For comparison, CNDR-51533 (cevipabulin)-treated cells demonstrated a significant reduction in α -tubulin at 100 nM, even though this concentration induced a significant increase in acetyl-tubulin levels (Supplemental Fig. 5). These results suggest CNDR-51657, and likely other TPD+ compounds, behave in a mechanistically distinct manner than TPD congeners bearing the alkoxy side-chain.

CNDR-51657 Increases Levels of Post-Translationally-Modified Tubulin in Cytoskeletal Cellular Fractions without Altering MT Morphology. To assess the effects of treatment with CNDR-51657 on the amount of free versus MT-incorporated tubulin, QBI-293 cells were treated with increasing doses of CNDR-51657 for 4 hours, followed by harvest under MT-stabilizing conditions. Soluble proteins were first extracted from cells adherent to the tissue culture dish in

MT-stabilizing buffer containing 1% Triton X-100 (“soluble” fraction). Under these conditions, the majority of the cytoskeleton, as well as the nuclei, remain bound to the tissue culture dish (Joshi and Cleveland, 1989). After extraction of soluble proteins, the remaining cytoskeleton was solubilized in 2% SDS-containing buffer (“cytoskeletal” fraction). Analysis of both fractions by immunoblotting revealed that nearly all of the post-translationally-modified tubulin was detected within the cytoskeletal/SDS fraction, as expected (Fig. 6A). Under these extraction conditions, α - and β -tubulin present in the soluble fraction represent free tubulin, whereas levels within the cytoskeletal fraction represent tubulin that has been incorporated into MTs. Treatment with 1 μ M or 10 μ M CNDR-51657, as well as with 0.1 μ M EpoD, significantly increased the levels of acetyl-tubulin in the cytoskeletal fraction (Fig. 6, A and C); the 10 μ M treatment with CNDR-51657, as well as EpoD, significantly increased levels of glu-tubulin (Fig. 6, A and C). Acetyl- and glu-tubulin were not detected within the soluble fraction at any dose of CNDR-51657, suggesting MTs remained intact (Fig. 6A). Additionally, significant increases in β -tubulin were observed within the cytoskeletal fraction following treatment with 1 or 10 μ M CNDR-51657 or 0.1 μ M EpoD (Fig. 6, A and C). The amount of α -tubulin within the cytoskeletal fraction was also slightly increased by 1 and 10 μ M CNDR-51657, although significance was only reached at the 1 μ M dose or with 0.1 μ M EpoD (Fig. 6, A and C). The increase in cytoskeletal tubulin was associated with a corresponding decrease in levels of α - and β -tubulin in the soluble fraction (Fig. 6, A and B). Collectively, these data suggest that TPD+ compounds such as CNDR-51657 cause redistribution of soluble tubulin to MTs, thereby increasing MT mass in a manner similar to the MT-stabilizing taxanes and epothilones (Schiff and Horwitz, 1980; Bollag et al., 1995).

To evaluate cytoskeletal architecture following treatment with CNDR-51657, COS-7 cells were treated for 4 hours with 1 μ M of the compound and MT structure was examined by

immunocytochemistry. An increase in acetylated tubulin was observed and the levels and distribution of β -tubulin did not appear to change relative to vehicle-treated cells, with normal MT structures (Fig. 6D). These findings are in contrast to what was observed at a similar concentration of CNDR-51555 (Fig. 2, A and B). At a 10 μ M dose of CNDR-51657, β -tubulin immunolabeling remained robust, although tubulin bundling appeared to occur around the nucleus (Fig. 6E), which was also observed upon treatment with 0.1 μ M EpoD (Fig. 2, A and B) and could be a result of mitotic block. The distribution of β -tubulin within the cells treated with 10 μ M of CNDR-51657 is substantially different than that observed within an identical concentration of CNDR-51555 or -51549 (Fig. 6E), with the latter compounds causing dramatic redistribution of β -tubulin, including the formation of punctate structures after treatment with CNDR-51555. These findings demonstrate that CNDR-51657 increases both markers of stable MTs and MT mass, characteristic of well-described MT-stabilizing compounds, and differs markedly in its activity relative to the structurally-related compounds CNDR-51555 and CNDR-51549.

CNDR-51657 Increases Markers of Stable MTs in Rat Primary Cortical Neurons without Disrupting Neuronal Morphology. As assessment of MT-stabilizing activity of the TPD and PPD compounds was performed only in dividing cells (QBI-293 and COS-7 cell lines), an evaluation of compound effects on the MTs of primary neurons was important to assess their potential for future testing in transgenic mouse models of tauopathy. Neuronal MTs serve as the major architectural framework for maintaining cellular morphology, and also serve as the railways for the transport of critical cellular proteins and organelles. Because neuronal MTs are highly stable under normal conditions within the brain and in mature neuronal culture systems, rat cortical neurons were assessed at a young age – 3 days in vitro (DIV) - when MTs tend to

JPET #231175

exhibit increased dynamicity compared to older cultures. Although CNDR-51555 and -51549 were shown to increase acetylated-tubulin in dividing cells at moderate concentrations, both compounds failed to increase acetyl-tubulin in primary neurons at the tested concentrations following 24 hours of treatment (Fig. 7A). In fact, acetyl-tubulin levels were significantly decreased by CNDR-51555 at 100 nM and 1 μ M, and by CNDR-51549 at 1 μ M (Fig. 7A). Similarly, there was a concomitant decrease in α -tubulin levels, as assessed by ELISA (Fig. 7B). Evidence of toxicity was observed after 10 μ M treatment with either compound, suggesting neurons may exhibit heightened sensitivity to these molecules. Due to the observed toxicity in the neuronal cultures, subsequent studies in primary neurons were conducted at concentrations not exceeding 1 μ M.

Unlike the results obtained following treatment of neurons with CNDR-51555 or -51549, ELISA results demonstrated that treatment of rat primary cortical neurons at 3 DIV with 1 μ M of CNDR-51657 for 24 hours induced a significant increase in acetyl-tubulin without a concomitant decrease in α -tubulin (Fig. 7C). The increase in acetyl-tubulin was similar in magnitude to that observed following treatment with the positive control, 100 nM EpoD (Fig. 7C). These results were confirmed by immunoblotting, which also demonstrated a significant increase in glu-tubulin with no change in total tubulin levels (Fig. 7, D and E). In contrast, both glu-tubulin and total tubulin amounts were decreased by treatment with CNDR-51555 or -51549 (Supplemental Fig. 6).

Levels of PTM- and total tubulin from neurons treated with CNDR-51657 were also assessed in the soluble and cytoskeletal fractions following harvest in MT-stabilizing buffer. Significantly increased acetyl- and glu-tubulin levels were observed in the cytoskeletal fraction from neurons treated at 3 DIV with 1 μ M CNDR-51657 or 0.1 μ M EpoD for 24 hours (Fig. 8, A

and C). Similar to the results obtained in QBI-293 cells, 1 μ M treatment with CNDR-51657 increased α - and β -tubulin levels in the cytoskeletal fraction, although only the increase in β -tubulin reached significance (Fig. 8, A and C). A concomitant decrease was observed in α - and β -tubulin levels in the soluble fraction, reaching significance for α -tubulin (Fig. 8, A and B). These findings again suggest TPD+ compounds, like EpoD, increase both MT stability and MT mass across multiple cell types.

Although CNDR-51657 and EpoD were only effective in increasing markers of stable MTs in young cultures (3 DIV), due to a majority of tubulin already being incorporated into MTs and post-translationally modified in older neuron cultures, we nonetheless examined the effects of compounds on more mature cultures in which processes and interneuronal connections have been more fully established. Rat primary cortical neurons at 7 DIV were examined by immunocytochemical staining with acetyl-tubulin antibody after 24 hour treatment with 1 μ M of CNDR-51657 or CNDR-51555. In comparison to vehicle-treated neurons, those exposed to CNDR-51555 for 24 hours demonstrated significant alterations in morphology and diminished acetyl-tubulin immunoreactivity (Fig. 8D). However, neurons treated with CNDR-51657 had a similar morphology to vehicle-treated neurons (Fig. 8D). Neurons treated with 100 nM EpoD also appeared similar to vehicle-treated neurons, although processes appeared slightly shorter and less branched (Fig. 8D), which could account for the slight decrease observed in total β -tubulin levels in whole-cell extracts from EpoD-treated neurons (Fig. 7, D and E). Overall, our findings suggest that TPD+ compounds, but not other TPD or PPD analogs, increase MT stabilization in primary neurons without significantly altering neuronal morphology or disrupting established networks.

CNDR-51657 Restores Neuronal MT Stability in Response to Tau Hyperphosphorylation

in Vitro. We have provided evidence that the TPD+ compound, CNDR-51657, can increase markers of MT stability in primary neuronal cultures. To evaluate whether this compound can stabilize neuronal MTs under conditions of tau loss-of-function, we treated rat primary cortical neurons (10 DIV) with okadaic acid (OA) in the absence or presence of CNDR-51657 for 8 hours. Okadaic acid potently inhibits the serine threonine protein phosphatases PP1 and PP2A (Bialojan and Takai, 1988), and treatment of neurons with OA has been shown to induce hyperphosphorylation of tau as well as decrease markers of MT stability, including acetylated tubulin (Merrick et al., 1997; Das and Miller, 2012). A significant increase in phosphorylated tau recognized by the AT8 antibody, which detects tau phosphorylated at serine 202 and threonine 205, confirms the efficacy of OA treatment (Fig. 9A). Furthermore, the reduction in acetyl- and glu-tubulin levels in OA-treated neurons demonstrates a loss of MTs that likely resulted from the disengagement of tau from MTs (Fig. 9, A and B). Although treatment of 10 DIV neurons for 8 h with 1 μ M CNDR-51657 alone had no effect on levels of post-translationally modified tubulin, co-administration of CNDR-51657 significantly attenuated the loss of acetyl- and glu-tubulin observed in OA-treated neurons (Fig. 9, A and B). Moreover, immunolabeling of acetyl-tubulin in these cultures demonstrated the preservation of both acetyl-tubulin levels and MT morphology in neurons treated dually with OA and CNDR-51657 when compared to OA treatment alone (Fig. 9C). These findings suggest that whereas TPD+ compounds have little effect on mature neurons in culture, they offer protection against MT loss and/or dysfunction under conditions of tau hyperphosphorylation and disengagement from MTs, as could occur in AD and related tauopathies. Conversely, treating neurons simultaneously with OA and CNDR-51555 or CNDR-51549 did not result in an inhibition of acetyl-tubulin loss induced by OA treatment

(Supplemental Fig. 7). Each of these compounds was administered at 100 nM, as higher concentrations of either compound was shown to reduce neuronal acetyl-tubulin (Fig. 7 and Supplemental Fig. 6). These studies further differentiate the CNDR-51657 and the TPD+ compounds from the other TPD and PPD examples.

CNDR-51657 Increases Acetyl-Tubulin in the Cortex of Wild-Type Mice. To examine the in vivo effects of CNDR-51657, wild-type CD-1 mice were administered two doses of 1 or 5 mg/kg -51657, approximately 18 h apart, by i.p. injection. Four hours after the second dose, mice were sacrificed and cortices were dissected for analysis of acetyl- and α -tubulin levels by ELISA. Acetyl-tubulin levels were significantly increased in both treatment groups compared to vehicle-treated animals (Fig. 10A). Alpha-tubulin levels were not significantly affected by either dose of CNDR-51657 (Fig. 10A). When the acetyl-tubulin: α -tubulin ratio was determined for each treatment group, a dose-dependent increase was observed (Fig. 10A). Past studies demonstrated an increase in the brain acetyl-tubulin: α -tubulin ratio of mice treated with the TPD CNDR-51555 daily for 4 or 6 days (Lou et al., 2014). To directly compare the efficacy of the TPD+ CNDR-51657 with that of the TPD CNDR-51555 in the current study, wild-type CD-1 mice were injected with 1 mg/kg CNDR-51657 or 1 or 5 mg/kg CNDR-51555 following the same dosing scheme as described above. Acetyl-tubulin levels were highest in cortices from mice treated with 1 mg/kg CNDR-51657, but an increase was also observed following treatment with 5 mg/kg, but not 1 mg/kg, CNDR-51555 (Fig. 10B). Alpha-tubulin levels were not significantly changed across groups, although a trend toward a decrease was observed in mice treated with CNDR-51555 (Fig. 10B). Interestingly, we previously observed a decrease in brain α -tubulin levels following 6 days treatment with CNDR-51549 or -51555, although at the time it was thought that this represented variability in the brain homogenates, as we were then unaware of the general

JPET #231175

phenotype of this compound class (unpublished data). The acetyl-tubulin:α-tubulin ratio was significantly increased in cortical tissue from mice treated with 1 mg/kg CNDR-51657 and 5 mg/kg CNDR-51555 (Fig. 10B). These studies suggest the TPD+ CNDR-51657 can elicit an in vivo pharmacodynamic effect on acetyl-tubulin levels without negatively affecting α-tubulin levels, and is also active in vivo at a lower dose than the previously disclosed TPD, CNDR-51555.

Discussion

Alzheimer's disease and related tauopathies are characterized by the formation of pathological aggregates composed of the MT-associated protein, tau. Hyperphosphorylation and fibrillization of tau are associated with a coincidental decrease in MT-bound tau, and there is evidence that this results in MT deficits in cell culture (Alonso et al., 1994; Merrick et al., 1997) and in tg mouse models of tauopathy (Zhang et al., 2005; Barten et al., 2012; Zhang et al., 2012). Moreover, there is evidence of MT deficits in AD brain, including decreased acetylated-tubulin (Hempfen and Brion, 1996) and a reduction in the total number and length of MTs within neurons (Cash et al., 2003). Recently, post-mortem evaluation of AD brain revealed decreased levels of total α -tubulin, in addition to a decreased acetylated and glu-tubulin, although there was no correlation between the presence of tangles and post-translationally modified tubulin within individual neurons. This is consistent with the idea that it is the initial hyperphosphorylation of tau and its disengagement from MTs that results in MT deficits (Zhang et al., 2015).

Neurons are particularly vulnerable to dysfunction resulting from MT instability, as they rely on MT networks both for architectural support and for the axonal transport of critical cellular proteins and organelles (Alonso et al., 1997; Baird and Bennett, 2013). Thus, the loss of tau function would be predicted to be detrimental to MT function and neuronal health, as supported by the aforementioned observations in AD brain. It was therefore somewhat surprising that genetic knock-out of murine tau was initially reported to result in no overt phenotype (Harada et al., 1994; Dawson et al., 2001). However, mounting evidence suggests that age-dependent MT and motor function deficits develop in tau-depleted mice (Dawson et al., 2010; Lopes et al., 2016). In addition, primary neurons derived from tau knock-out mice show impaired neurite outgrowth (Dawson et al., 2001). Finally, up-regulation of additional microtubule-

associated proteins, such as MAP1A, has been observed in tau knock-out models (Harada et al., 1994), hampering the ability to discern the full effect of tau loss-of-function. Transgenic over-expression models have provided additional means to explore the consequences of tau hyperphosphorylation and the accumulation of pathological tau. Indeed, our laboratory has shown that tau tg mice exhibit MT deficits, axonal dystrophy, behavioral impairments, neuron loss and shortened life span (Ballatore et al., 2007; Brunden et al., 2012; Yoshiyama et al., 2013), which recapitulates many features of AD and related tauopathies. Although therapeutic strategies in AD have traditionally focused on lowering amyloid-beta ($A\beta$) extracellular plaque load, tau pathology has received increasing attention over recent years, given that the levels of neurofibrillary tangles correlate more closely with cognitive decline than amyloid plaque burden (Wilcock and Esiri, 1982; Arriagada et al., 1992; Gómez-Isla et al., 1997). In this context, multiple approaches are being investigated that are aimed at reducing tau hyperphosphorylation or misfolded tau species (Brunden et al., 2009; Lee et al., 2011). An alternate approach is to target tau loss-of-function. In this context, our group (Brunden et al., 2010; Zhang et al., 2012) and others (Barten et al., 2012) have demonstrated in tg mouse models of brain tauopathy that the MT-stabilizing compound, EpoD, exerts improvements in MT and axonal function that result in reduced neurodegeneration and enhanced cognitive function. The observation that EpoD-treated tau tg mice also had reduced tau pathology (Barten et al., 2012; Zhang et al., 2012) suggests that MT dysfunction contributes to the deposition of insoluble tau or the inability of diseased cells to clear toxic tau aggregates.

Here, we have described the biochemical properties of a series of non-naturally occurring MT-binding compounds that had been originally identified as potential anti-fungal agents, and then later developed as candidate cancer chemotherapeutics (Zhang et al., 2007; Zhang et al.,

2009). An in-depth analysis of several TPD and PPD congeners (Lou et al., 2014) reveals interesting new elements of structure-activity relationship that led to the identification of two distinct groups of compounds based on the particular cellular phenotype elicited. Whereas active PPDs and TPDs bearing an alkoxy side-chain in the para-position promoted both an increase in markers of stable MTs and degradation of tubulin in a proteasome-dependent manner, the active TPD congeners lacking the alkoxy side-chain did not decrease total tubulin levels or affect MT architecture. These “TPD+” small molecules induced concentration-dependent increases in markers of stable MTs and increased MT mass without obvious morphological alteration to existing MT networks. Moreover, the prototype TPD+ small molecule, CNDR-51657, is brain-penetrant, orally bioavailable and stabilizes MTs in primary neurons and in mouse brain after peripheral administration. Given these desirable properties, the TPD+ compounds represent a new class of potential candidate drugs for the treatment of neurodegenerative tauopathies.

Although the changes in MT structure and the reduction of tubulin levels caused by certain TPD compounds, exemplified by CNDR-51555, and by all tested PPDs indicate that these compounds would not be beneficial for the treatment of tauopathies, it is possible that these effects may prove useful in an oncology setting, particularly in glioblastoma, a highly fatal condition where traditional therapeutics have failed to achieve sufficient brain exposure (Katsetos et al., 2015; van Tellingen et al., 2015). Although we do not fully understand why many of the TPD and PPD compounds induce proteasomal degradation of tubulin, one hypothesis is that these compounds promote the formation of aberrant or unstable MT structures. The promotion of anomalous MT structures that are subject to proteolysis would be consistent with the observed increase of acetyl-tubulin and glu-tubulin at concentrations in which reductions of total tubulin are also observed. The finding that TPD+ compounds increase

markers of stable MT in the absence of tubulin degradation suggests that the nature of the substituent in the para position may ultimately determine the nature of the MT structure that forms, with TPD+ compounds lacking an alkoxy moiety inducing normal MTs that are no longer targeted for removal.

The ability of the TPD+ prototype, CNDR-51657, to increase markers of stable MTs in primary neurons without evidence of tubulin degradation is highly significant, especially since other PPD and TPD compounds which increased markers of stable MTs in QBI-293 cells failed to increase these markers in neurons. Importantly, CNDR-51657 was shown to increase MT mass within QBI-293 cells and neurons, and thus mimicked in many ways the effects of EpoD in these cells. Furthermore, treatment of older neuronal cultures (7 DIV) that have more mature neuritic processes with CNDR-51657 did not appear to alter neuronal morphology or disrupt existing MT networks in our culture systems. This contrasts dramatically with the effect of the related TPD, CNDR-51555, which caused significant MT disruption and truncation of neuritic processes. Finally, CNDR-51657 was able to alleviate MT deficits in neurons treated with OA, an in vitro model of tau hyperphosphorylation with associated loss of stable MTs, whereas CNDR-51555 was not.

In summary, we have characterized a number of small molecules containing PPD and TPD core structures and have demonstrated differential effects on cellular MTs that can be related to certain structural features of the compounds. A preferred set of TPD+ small molecules exhibit MT-stabilizing properties in multiple cell types, including primary neurons. Moreover, several examples from this class were found to penetrate the BBB and have excellent brain exposure, and importantly, CNDR-51657 was shown to increase acetylated-tubulin in mouse

JPET #231175

brain after peripheral administration. Thus, these compounds, as exemplified by CNDR-51657, hold promise as potential candidates for the treatment of tauopathies.

Acknowledgements

The authors thank Amy Lam and Sarah DeVaro for their laboratory assistance. We would like to acknowledge the following donors to the Center for Neurodegenerative Disease Research: the Karen Cohen Segal and Christopher S. Segal Alzheimer Drug Discovery Initiative Fund, the Paula C. Schmerler Fund for Alzheimer's Research, the Barrist Neurodegenerative Disease Research Fund, the Eleanor Margaret Kurtz Endowed Fund, the Mary Rasmus Endowed Fund for Alzheimer's Research, Mrs. Gloria J. Miller and Arthur Peck, M.D.

JPET #231175

Authorship Contributions

Participated in research design: Kovalevich, Cornec, Lee, Smith III, Ballatore, and Brunden.

Conducted experiments: Kovalevich, Cornec, Yao, James, Crowe

Contributed new reagents or analytical tools: N/A

Performed data analysis: Kovalevich, James, and Crowe

Wrote or contributed to the writing of the manuscript: Kovalevich, Cornec, James, Lee, Trojanowski, Smith III, Ballatore, and Brunden.

References

- Alonso AC, Zaidi T, Grundke-Iqbal I and Iqbal K (1994) Role of abnormally phosphorylated tau in the breakdown of microtubules in Alzheimer disease. *Proc Natl Acad Sci U S A* **91**:5562-5566.
- Alonso AD, Grundke-Iqbal I, Barra HS and Iqbal K (1997) Abnormal phosphorylation of tau and the mechanism of Alzheimer neurofibrillary degeneration: sequestration of microtubule-associated proteins 1 and 2 and the disassembly of microtubules by the abnormal tau. *Proc Natl Acad Sci U S A* **94**:298-303.
- Arriagada PV, Growdon JH, Hedley-Whyte ET and Hyman BT (1992) Neurofibrillary tangles but not senile plaques parallel duration and severity of Alzheimer's disease. *Neurology* **42**:631-639.
- Baird FJ and Bennett CL (2013) Microtubule defects & Neurodegeneration. *J Genet Syndr Gene Ther* **4**:203.
- Ballatore C, Brunden KR, Huryn DM, Trojanowski JQ, Lee VMY and Smith AB (2012) Microtubule Stabilizing Agents as Potential Treatment for Alzheimer's Disease and Related Neurodegenerative Tauopathies. *Journal of Medicinal Chemistry* **55**:8979-8996.
- Ballatore C, Lee VM and Trojanowski JQ (2007) Tau-mediated neurodegeneration in Alzheimer's disease and related disorders. *Nat Rev Neurosci* **8**:663-672.
- Barten DM, Fanara P, Andorfer C, Hoque N, Wong PYA, Husted KH, Cadelina GW, Decarr LB, Yang L, Liu V, Fessler C, Protassio J, Riff T, Turner H, Janus CG, Sankaranarayanan S, Polson C, Meredith JE, Gray G, Hanna A, Olson RE, Kim SH, Vite GD, Lee FY and Albright CF (2012) Hyperdynamic Microtubules, Cognitive Deficits, and Pathology Are Improved in Tau Transgenic Mice with Low Doses of the Microtubule-Stabilizing Agent BMS-241027. *Journal of Neuroscience* **32**:7137-7145.
- Beyer CF, Zhang N, Hernandez R, Vitale D, Lucas J, Nguyen T, Discafani C, Ayral-Kaloustian S and Gibbons JJ (2008) TTI-237: a novel microtubule-active compound with in vivo antitumor activity. *Cancer Res* **68**:2292-2300.
- Beyer CF, Zhang N, Hernandez R, Vitale D, Nguyen T, Ayral-Kaloustian S and Gibbons JJ (2009) The microtubule-active antitumor compound TTI-237 has both paclitaxel-like and vincristine-like properties. *Cancer Chemother Pharmacol* **64**:681-689.
- Bialojan C and Takai A (1988) Inhibitory effect of a marine-sponge toxin, okadaic acid, on protein phosphatases. Specificity and kinetics. *Biochem J* **256**:283-290.
- Bollag DM, McQueney PA, Zhu J, Hensens O, Koupal L, Liesch J, Goetz M, Lazarides E and Woods CM (1995) Epopothilones, a new class of microtubule-stabilizing agents with a taxol-like mechanism of action. *Cancer Res* **55**:2325-2333.
- Brunden KR, Ballatore C, Lee VM, Smith AB, 3rd and Trojanowski JQ (2012) Brain-penetrant microtubule-stabilizing compounds as potential therapeutic agents for tauopathies. *Biochem Soc Trans* **40**:661-666.
- Brunden KR, Trojanowski JQ and Lee VMY (2009) Advances in tau-focused drug discovery for Alzheimer's disease and related tauopathies. *Nature Reviews Drug Discovery* **8**:783-793.
- Brunden KR, Yao Y, Potuzak JS, Ferrer NI, Ballatore C, James MJ, Hogan AM, Trojanowski JQ, Smith AB and Lee VM (2011) The characterization of microtubule-stabilizing drugs as possible therapeutic agents for Alzheimer's disease and related tauopathies. *Pharmacol Res* **63**:341-351.

- Brunden KR, Zhang B, Carroll J, Yao Y, Potuzak JS, Hogan AML, Iba M, James MJ, Xie SX, Ballatore C, Smith AB, III, Lee VMY and Trojanowski JQ (2010) Epothilone D improves microtubule density, axonal integrity and cognition in a transgenic mouse model of tauopathy. *Journal of Neuroscience* **30**:13861-13866.
- Cash AD, Aliev G, Siedlak SL, Nunomura A, Fujioka H, Zhu XW, Raina AK, Vinters HV, Tabaton M, Johnson AB, Paula-Barbosa M, Avila J, Jones PK, Castellani RJ, Smith MA and Perry G (2003) Microtubule reduction in Alzheimer's disease and aging is independent of tau filament formation. *American Journal of Pathology* **162**:1623-1627.
- Cornec AS, James MJ, Kovalevich J, Trojanowski JQ, Lee VM, Smith AB, Ballatore C and Brunden KR (2015) Pharmacokinetic, pharmacodynamic and metabolic characterization of a brain retentive microtubule (MT)-stabilizing triazolopyrimidine. *Bioorg Med Chem Lett* **25**:4980-4982.
- Das V and Miller JH (2012) Microtubule stabilization by peloruside A and paclitaxel rescues degenerating neurons from okadaic acid-induced tau phosphorylation. *Eur J Neurosci* **35**:1705-1717.
- Dawson HN, Cantillana V, Jansen M, Wang H, Vitek MP, Wilcock DM, Lynch JR and Laskowitz DT (2010) Loss of Tau Elicits Axonal Degeneration in A Mouse Model of Alzheimer's Disease. *Neuroscience* **169**:516-531.
- Dawson HN, Ferreira A, Eyster MV, Ghoshal N, Binder LI and Vitek MP (2001) Inhibition of neuronal maturation in primary hippocampal neurons from tau deficient mice. *J Cell Sci* **114**:1179-1187.
- Demasi M and Davies KJ (2003) Proteasome inhibitors induce intracellular protein aggregation and cell death by an oxygen-dependent mechanism. *FEBS Lett* **542**:89-94.
- Gómez-Isla T, Hollister R, West H, Mui S, Growdon JH, Petersen RC, Parisi JE and Hyman BT (1997) Neuronal loss correlates with but exceeds neurofibrillary tangles in Alzheimer's disease. *Ann Neurol* **41**:17-24.
- Harada A, Oguchi K, Okabe S, Kuno J, Terada S, Ohshima T, Satoyoshitake R, Takei Y, Noda T and Hirokawa N (1994) Altered Microtubule Organization in Small-Caliber Axons of Mice Lacking Tau-Protein. *Nature* **369**:488-491.
- Hempen B and Brion JP (1996) Reduction of acetylated alpha-tubulin immunoreactivity in neurofibrillary tangle-bearing neurons in Alzheimer's disease. *Journal of Neuropathology and Experimental Neurology* **55**:964-972.
- Huff LM, Sackett DL, Poruchynsky MS and Fojo T (2010) Microtubule-disrupting chemotherapeutics result in enhanced proteasome-mediated degradation and disappearance of tubulin in neural cells. *Cancer Res* **70**:5870-5879.
- Joshi HC and Cleveland DW (1989) Differential utilization of beta-tubulin isotypes in differentiating neurites. *J Cell Biol* **109**:663-673.
- Katsetos CD, Reginato MJ, Baas PW, D'Agostino L, Legido A, Tuszynski JA, Dráberová E and Dráber P (2015) Emerging microtubule targets in glioma therapy. *Semin Pediatr Neurol* **22**:49-72.
- Kreis TE (1987) Microtubules containing detyrosinated tubulin are less dynamic. *EMBO J* **6**:2597-2606.
- Lecker SH, Goldberg AL and Mitch WE (2006) Protein degradation by the ubiquitin-proteasome pathway in normal and disease states. *J Am Soc Nephrol* **17**:1807-1819.
- Lee CB, Wu Z, Zhang F, Chappell MD, Stachel SJ, Chou TC, Guan Y and Danishefsky SJ (2001a) Insights into long-range structural effects on the stereochemistry of aldol

- condensations: a practical total synthesis of desoxyepothilone F. *J Am Chem Soc* **123**:5249-5259.
- Lee VM, Brunden KR, Hutton M and Trojanowski JQ (2011) Developing therapeutic approaches to tau, selected kinases, and related neuronal protein targets. *Cold Spring Harb Perspect Med* **1**:a006437.
- Lee VM, Goedert M and Trojanowski JQ (2001b) Neurodegenerative tauopathies. *Annu Rev Neurosci* **24**:1121-1159.
- Lopes S, Lopes A, Pinto V, Guimarães MR, Sardinha VM, Duarte-Silva S, Pinheiro S, Pizarro J, Oliveira JF, Sousa N, Leite-Almeida H and Sotiropoulos I (2016) Absence of Tau triggers age-dependent sciatic nerve morphofunctional deficits and motor impairment. *Aging Cell*.
- Lou K, Yao Y, Hoyer AT, James MJ, Cornec AS, Hyde E, Gay B, Lee VM, Trojanowski JQ, Smith AB, Brunden KR and Ballatore C (2014) Brain-penetrant, orally bioavailable microtubule-stabilizing small molecules are potential candidate therapeutics for Alzheimer's disease and related tauopathies. *J Med Chem* **57**:6116-6127.
- Merrick SE, Trojanowski JQ and Lee VMY (1997) Selective destruction of stable microtubules and axons by inhibitors of protein serine/threonine phosphatases in cultured human neurons (NT2N cells). *Journal of Neuroscience* **17**:5726-5737.
- Mi L, Gan N, Cheema A, Dakshanamurthy S, Wang X, Yang DC and Chung FL (2009a) Cancer preventive isothiocyanates induce selective degradation of cellular alpha- and beta-tubulins by proteasomes. *J Biol Chem* **284**:17039-17051.
- Mi L, Gan N and Chung FL (2009b) Aggresome-like structure induced by isothiocyanates is novel proteasome-dependent degradation machinery. *Biochem Biophys Res Commun* **388**:456-462.
- Mizushima N and Komatsu M (2011) Autophagy: renovation of cells and tissues. *Cell* **147**:728-741.
- Rivkin A, Yoshimura F, Gabarda AE, Cho YS, Chou TC, Dong H and Danishefsky SJ (2004) Discovery of (E)-9,10-dehydroepothilones through chemical synthesis: on the emergence of 26-trifluoro-(E)-9,10-dehydro-12,13-desoxyepothilone B as a promising anticancer drug candidate. *J Am Chem Soc* **126**:10913-10922.
- Schiff PB and Horwitz SB (1980) Taxol stabilizes microtubules in mouse fibroblast cells. *Proc Natl Acad Sci U S A* **77**:1561-1565.
- Schulze E, Asai DJ, Bulinski JC and Kirschner M (1987) Posttranslational modification and microtubule stability. *J Cell Biol* **105**:2167-2177.
- van Tellingen O, Yetkin-Arik B, de Gooijer MC, Wesseling P, Wurdinger T and de Vries HE (2015) Overcoming the blood-brain tumor barrier for effective glioblastoma treatment. *Drug Resist Updat* **19**:1-12.
- Wibo M and Poole B (1974) Protein degradation in cultured cells. II. The uptake of chloroquine by rat fibroblasts and the inhibition of cellular protein degradation and cathepsin B1. *J Cell Biol* **63**:430-440.
- Wilcock GK and Esiri MM (1982) Plaques, tangles and dementia. A quantitative study. *J Neurol Sci* **56**:343-356.
- Wood JG, Mirra SS, Pollock NJ and Binder LI (1986) Neurofibrillary tangles of Alzheimer disease share antigenic determinants with the axonal microtubule-associated protein tau (tau). *Proc Natl Acad Sci U S A* **83**:4040-4043.

- Yoshiyama Y, Higuchi M, Zhang B, Huang SM, Iwata N, Saido TC, Maeda J, Suhara T, Trojanowski JQ and Lee VMY (2007) Synapse loss and microglial activation precede tangles in a P301S tauopathy mouse model. *Neuron* **53**:337-351.
- Yoshiyama Y, Lee VM and Trojanowski JQ (2013) Therapeutic strategies for tau mediated neurodegeneration. *J Neurol Neurosurg Psychiatry* **84**:784-795.
- Zhang B, Carroll J, Trojanowski JQ, Yao Y, Iba M, Potuzak JS, Hogan AL, Xie SX, Smith AB, III, Lee VMY and Brunden KR (2012) The microtubule-stabilizing agent, epothilone D, reduces axonal dysfunction, cognitive deficits, neurotoxicity and Alzheimer-like pathology in an interventional study with aged tau transgenic mice *Journal of Neuroscience* **32**:3601-3611.
- Zhang B, Maiti A, Shively S, Lakhani F, McDonald-Jones G, Bruce J, Lee EB, Xie SX, Joyce S, Li C, Toleikis PM, Lee VM and Trojanowski JQ (2005) Microtubule-binding drugs offset tau sequestration by stabilizing microtubules and reversing fast axonal transport deficits in a tauopathy model. *Proc Natl Acad Sci U S A* **102**:227-231.
- Zhang F, Su B, Wang C, Siedlak SL, Mondragon-Rodriguez S, Lee HG, Wang X, Perry G and Zhu X (2015) Posttranslational modifications of α -tubulin in alzheimer disease. *Transl Neurodegener* **4**:9.
- Zhang N, Ayrar-Kaloustian S, Nguyen T, Afragola J, Hernandez R, Lucas J, Gibbons J and Beyer C (2007) Synthesis and SAR of [1,2,4]triazolo[1,5-a]pyrimidines, a class of anticancer agents with a unique mechanism of tubulin inhibition. *J Med Chem* **50**:319-327.
- Zhang N, Ayrar-Kaloustian S, Nguyen T, Hernandez R, Lucas J, Discafani C and Beyer C (2009) Synthesis and SAR of 6-chloro-4-fluoroalkylamino-2-heteroaryl-5-(substituted)phenylpyrimidines as anti-cancer agents. *Bioorg Med Chem* **17**:111-118.

JPET #231175

Footnotes

€This work was supported by the National Institute of Health, National Institute on Aging [Grant AG044332] and in part by the Marian S. Ware Alzheimer Foundation.

Figure Legends

Fig 1. High doses of prototype TPD and PPD compounds induce loss of post-translationally-modified and total tubulin in QBI-293 Cells. (A) ELISA measuring acetyl-tubulin levels in response to 4 h treatment with TPD (CNDR-51555) or PPD (CNDR-51549). (B) ELISA measuring α -tubulin levels in response to 4 h treatment with CNDR-51555 or CNDR-51549. (C) Representative immunoblot for acetyl-, glu-, α -, and β -tubulin levels in QBI-293 lysates following 4 h treatment with CNDR-51555. (D) Quantification of tubulin levels from immunoblots of QBI-293 cell lysates following treatment with CNDR-51555. Loading controls GAPDH or β -actin were used for normalization. (E) Representative immunoblot for acetyl-, glu-, α -, and β -tubulin levels in QBI-293 lysates following 4 h treatment with CNDR-51549. (F) Quantification of tubulin levels from immunoblots of QBI-293 cell lysates following treatment with CNDR-51549. Loading controls GAPDH or β -actin were used for normalization. Data are representative of three independent experiments (n=3 per group). *p<0.05; **p<0.01; ***p<0.001 compared to vehicle (DMSO)-treated controls.

Fig 2. Immunocytochemistry in COS-7 cells reveals that the prototype TPD, CNDR-51555, induces concentration-dependent loss of β -tubulin immunoreactivity and disruption of MT networks. (A) Acetyl- and β -tubulin double-immunolabeling in COS-7 cells treated for 4 h with vehicle (DMSO; control), 100 nM EpoD, or 1 or 10 μ M of CNDR-51555. Nuclei are labeled blue with DAPI. 20X magnification; scale bar = 200 μ m. (B) Higher magnification of β -tubulin immunolabeling from boxed regions in “A”.

Fig 3. Inhibition of autophagy by chloroquine (CQ) administration does not rescue TPD- and PPD-mediated loss of tubulin in QBI-293 Cells. (A) ELISA measuring α -tubulin levels in

response to 4 h treatment with CNDR-51555 or CNDR-51549 in the absence or presence of 100 μ M CQ. (B) Representative immunoblot and quantification of β -tubulin levels following 4 h treatment with CNDR-51555 in the absence or presence of CQ. (C) Representative immunoblot and quantification of β -tubulin levels following 4 h treatment with CNDR-51549 in the absence or presence of CQ. β -tubulin levels were normalized to the loading control, β -actin. Data are representative of three independent experiments (n=3 per group). *p<0.05; ***p<0.001 compared to vehicle (DMSO)-treated controls, and †p<0.05 between indicated groups.

Fig 4. Inhibition of the proteasome by MG-132 administration rescues TPD- and PPD-mediated loss of tubulin in QBI-293 cells, with “rescued” tubulin largely redistributed to the RIPA-insoluble cellular fraction. (A) ELISA measuring α -tubulin levels in the RIPA-soluble fraction following 4 h treatment with CNDR-51555 or CNDR-51549 in the absence or presence of 10 μ M MG-132. (B) Immunoblot demonstrating accumulation of ubiquitinated proteins in response to MG-132 treatment. (C) Representative immunoblot of α - and β -tubulin within the RIPA-insoluble fraction following 4 h treatment with CNDR-51555 in the absence or presence of MG-132. (D) Representative immunoblot of α - and β -tubulin within the RIPA-insoluble fraction following 4 h treatment with CNDR-51549 in the absence or presence of MG-132. (E) Representative immunoblot of α - and β -tubulin in samples containing equal proportions of lysate from RIPA-soluble and SDS-soluble cellular fractions following 4 h treatment with CNDR-51555 in the absence or presence of MG-132. (F) Quantification of tubulin levels after immunoblot analysis of lysates containing equal proportions of RIPA-soluble and SDS-soluble fractions following 4 h treatment with CNDR-51555 in the absence or presence of MG-132. Tubulin levels were normalized to loading controls, GAPDH or β -actin. (G) Representative immunoblot of α - and β -tubulin in samples containing equal proportions of lysate from RIPA-

soluble and SDS-soluble cellular fractions following 4 h treatment with CNDR-51549 in the absence or presence of MG-132. (H) Quantification of tubulin levels after immunoblot analysis of lysates containing equal proportions of RIPA-soluble and SDS-soluble fractions following 4 h treatment with CNDR-51549 in the absence or presence of MG-132. Tubulin levels were normalized to loading controls, GAPDH or β -actin. Data are representative of three independent experiments (n=3 per group). **p<0.01; ***p<0.001 compared to vehicle (DMSO)-treated controls, and †††p<0.001 between indicated groups.

Fig 5. TPD+ compounds induce concentration-dependent increases in acetyl-tubulin levels without reducing α - and β -tubulin. (A) ELISA measuring acetyl- or α -tubulin levels in response to 4 h treatment with CNDR-51597. (B) ELISA measuring acetyl- or α -tubulin levels in response to 4 h treatment with CNDR-51657. (C) Representative immunoblot for acetyl-, glu-, α -, and β -tubulin levels in QBI-293 lysates following 4 h treatment with CNDR-51657. (D) Quantification of tubulin levels after immunoblot analysis of QBI-293 cell lysates following treatment with CNDR-51657. Tubulin levels were normalized to loading controls, GAPDH or β -actin. Data are representative of three independent experiments (n=3 per group). *p<0.05; ***p<0.001 compared to vehicle (DMSO)-treated controls.

Fig 6. The TPD+ compound, CNDR-51657, increases MT mass in QBI-293 cells without disrupting MT morphology. (A) Representative immunoblot of acetyl-, glu-, α -, and β -tubulin in the soluble and cytoskeletal fractions from QBI-293 cells following 4 h treatment with CNDR-51657. (B) Quantification of tubulin levels after immunoblot analysis of the soluble cellular fraction following 4 h treatment with CNDR-51657. Tubulin levels were normalized to the loading control, GAPDH. (C) Quantification of tubulin levels after immunoblot analysis of the cytoskeletal cellular fraction following 4 h treatment with CNDR-51657. Tubulin levels were

normalized to the loading control, Histone 3. (D) Representative acetyl- and β -tubulin immunolabeling in COS-7 cells treated with vehicle (DMSO; control) or 1 μ M CNDR-51657. Nuclei are labeled blue with DAPI. (E) Representative β -tubulin images in COS-7 cells treated with 10 μ M of CNDR-51657, -51555, or -51549. 40X magnification; scale bar = 100 μ m. Data are representative of three independent experiments (n=2-3 per group). *p<0.05; **p<0.01; ***p<0.001 compared to vehicle (DMSO)-treated controls.

Fig 7. The TPD+ compound, CNDR-51657, increases markers of stable MTs in rat cortical neurons, while other TPD and PPD compounds reduce total tubulin without increasing markers of stable MTs. (A) ELISA measuring acetyl-tubulin levels in rat cortical neurons following 24 h treatment with CNDR-51555 or -51549. (B) ELISA measuring α -tubulin levels in rat cortical neurons following 24 h treatment with CNDR-51555 or -51549. (C) ELISA measuring acetyl- and α -tubulin levels in rat cortical neurons following 24 h treatment with CNDR-51657. (D) Representative immunoblot of acetyl-, glu-, α -, and β -tubulin levels in rat cortical neurons after 24 h treatment with CNDR-51657. (E) Quantification of tubulin levels after immunoblot analysis of rat cortical neuron homogenates after 24 h treatment with CNDR-51657. Tubulin levels were normalized to β -actin. Data are representative of three independent experiments (n=3 per group). *p<0.05; **p<0.01; ***p<0.001 compared to vehicle (DMSO)-treated controls.

Fig 8. The TPD+ compound CNDR-51657 increases post-translationally modified tubulin and MT mass in rat cortical neurons without disrupting MT morphology. (A) Representative immunoblot of acetyl-, glu-, α -, and β -tubulin in the soluble and cytoskeletal fractions from rat cortical neurons (3 DIV) following 24 h treatment with CNDR-51657. (B) Quantification of tubulin levels after immunoblot analysis of the soluble cellular fraction following 24 h treatment with CNDR-51657. Tubulin levels were normalized to GAPDH. (C) Quantification of tubulin

JPET #231175

levels after immunoblot analysis of the cytoskeletal cellular fraction following 24 h treatment with CNDR-51657. Tubulin levels were normalized to Histone 3. (D) Representative acetyl-tubulin immunolabeling in rat cortical neurons (7 DIV) treated with vehicle (DMSO; control), 100 nM EpoD, 1 μ M CNDR-51657, or 1 μ M CNDR-51555. Nuclei are labeled blue with DAPI. Top row shows 10X magnification images; scale bar = 200 μ m. Bottom row shows 40X magnification images; scale bar = 100 μ m. Data are representative of three independent experiments (n=3 per group). *p<0.05; **p<0.01; ***p<0.001 compared to vehicle (DMSO)-treated controls.

Fig 9. The TPD+ compound CNDR-51657 restores MT stability in response to tau hyperphosphorylation in primary neurons. (A) Representative immunoblot of phosphorylated tau (AT8), acetyl-tubulin, and glu-tubulin in whole-cell lysates from rat cortical neurons (10 DIV) treated for 8 h with CNDR-51657, OA, or CNDR-51657 + OA. (B) Quantification of acetyl- and glu-tubulin levels after immunoblot analysis of neuronal lysates following 8 h treatment with CNDR-51657, OA, or CNDR-51657 + OA. Protein levels were normalized to beta-actin. (C) Representative acetyl-tubulin immunolabeling in rat cortical neurons (10 DIV) treated with vehicle (DMSO; control), OA, or OA + CNDR-51657 for 8 h. Nuclei are labeled blue with DAPI. Top row shows 10X magnification images; scale bar = 200 μ m. Bottom row shows 40X magnification images; scale bar = 100 μ m. Data are representative of three independent experiments (n=2-3 per group). **p<0.01; ***p<0.001 compared to vehicle (DMSO)-treated controls, and †††p<0.001 between indicated groups.

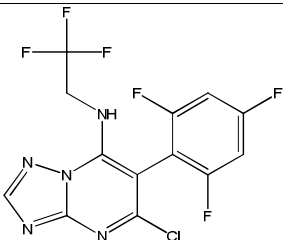
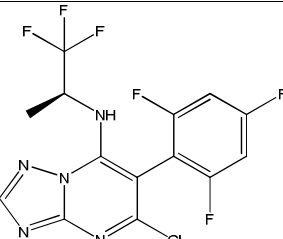
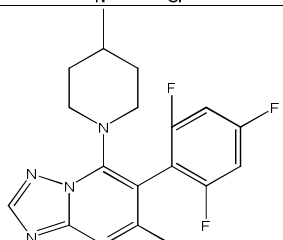
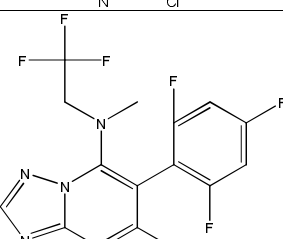
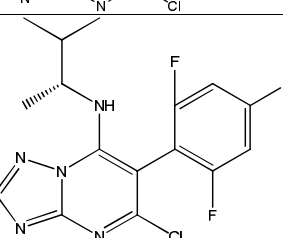
Fig 10. The TPD+ compound CNDR-51657 increases acetyl-tubulin levels in the cortex of WT mice. (A) ELISA analysis of acetyl- and α -tubulin levels in cortical tissue from mice treated with 1 or 5 mg/kg CNDR-51657. Mice received i.p. injections of vehicle (DMSO) or compound twice

JPET #231175

in a 24 h period, and brains were harvested 4 h after the second dose. (B) ELISA analysis of acetyl- and α -tubulin levels in cortical tissue from mice treated with 1 mg/kg CNDR-51657 or 1 or 5 mg/kg of the TPD CNDR-51555. Mice received i.p. injections of vehicle (DMSO) or compound twice in a 24 h period, and brains were harvested 4 h after the second dose. Bars represent average values normalized to vehicle-treated controls \pm S.E.M. Results were analyzed by one-way ANOVA with Dunnett's post-hoc testing where applicable (n =3 per group for each experiment).

Tables

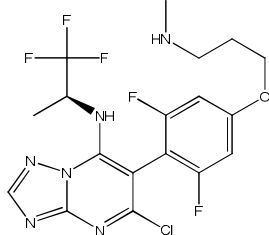
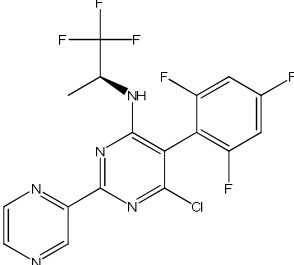
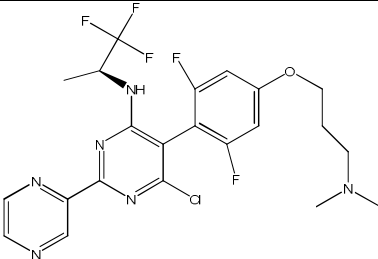
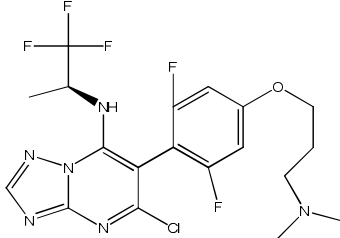
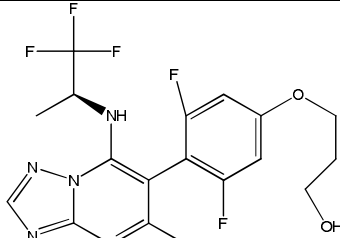
Table 1. List of TPD+ Compounds – Structure and Activity in the Acetyl-Tubulin ELISA

ID	Structure	Acetyl-Tubulin Change at 1 μM^*	Acetyl-Tubulin Change at 10 μM^*	B/P ratio**
CNDR-51539		3.07 (0.53)	3.38 (0.58)	1.1 (726 nM)
CNDR-51597		2.45 (0.38)	4.92 (0.77)	0.8 (2394 nM)
CNDR-51647		2.22 (0.57)	3.71 (0.94)	3.5 (228 nM)
CNDR-51655		1.68 (0.35)	2.69 (0.56)	6.7 (340 nM)
CNDR-51657		2.42 (0.49)	3.9 (0.79)	2.7 (812 nM)

*value represents fold-change over control (DMSO)-treated cells; number in parenthesis represents fold-change over 100 nM CNDR-51533-treated cells

**value represents brain-to-plasma ratio of drug 1 h after 5 mg/kg i.p. injection; number in parenthesis represents brain exposure

Table 2. List of example PPD and TPD Compounds – Structure and Activity in Acetyl-Tubulin ELISA

ID	Structure	Acetyl-Tubulin Change at 1 μM*	Acetyl-Tubulin Change at 10 μM*	Dose(s) Alpha-Tubulin Decreased
CNDR-51533		7.07 (1.29)	0.10 (0.02)	100 nM 1 μM 10 μM
CNDR-51549		4.77 (1.05)	1.37 (0.30)	1 μM 10 μM
CNDR-51554		4.19 (0.77)	0.53 (0.10)	100 nM 1 μM 10 μM
CNDR-51555		6.02 (1.34)	0.53 (0.17)	100 nM 1 μM 10 μM
CNDR-51567		7.01 (1.29)	1.18 (0.22)	1 μM 10 μM

*value represents fold-change over control (DMSO)-treated cells; number in parenthesis represents fold-change over 100 nM CNDR-51533-treated cells

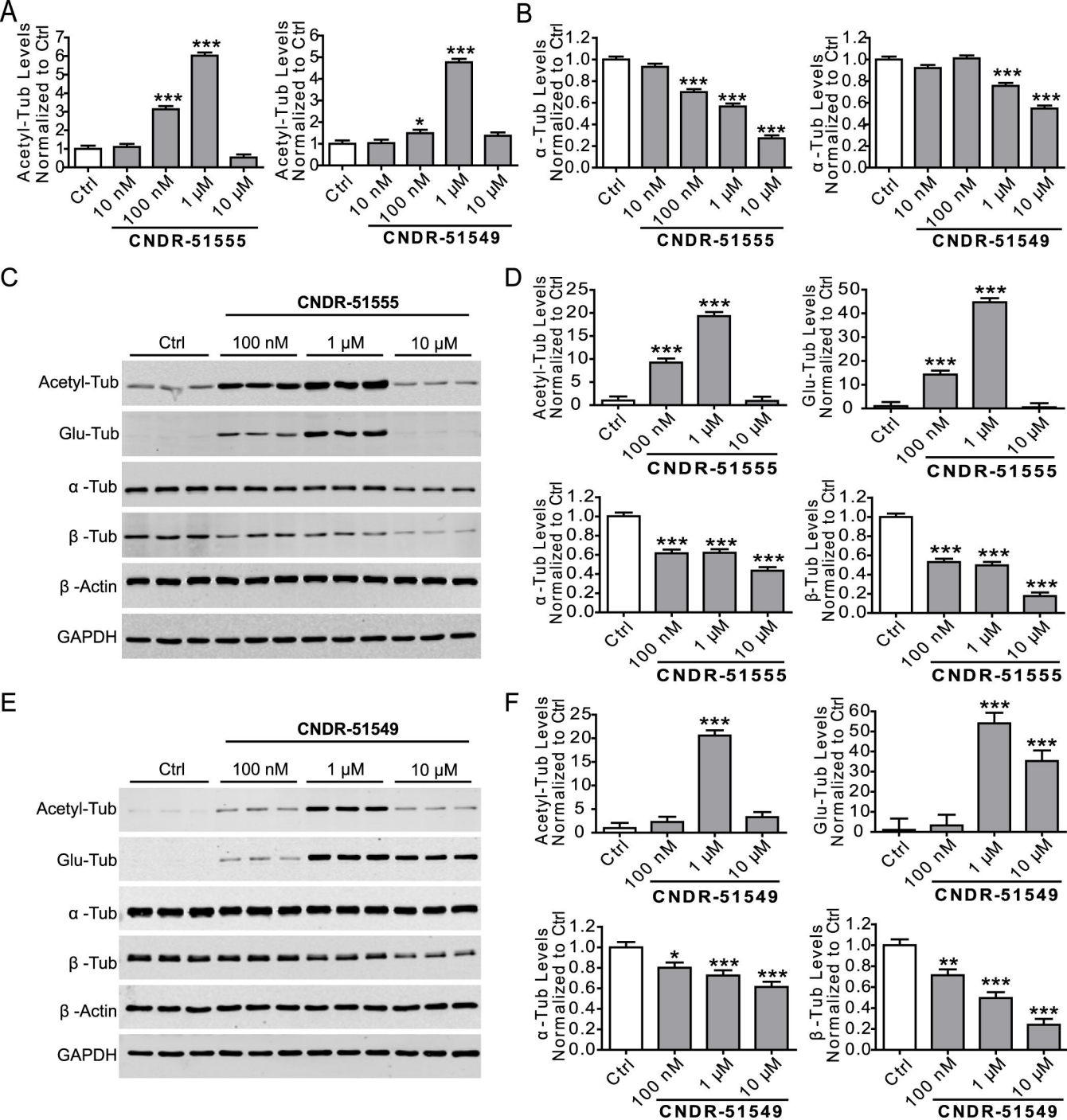


Figure 1

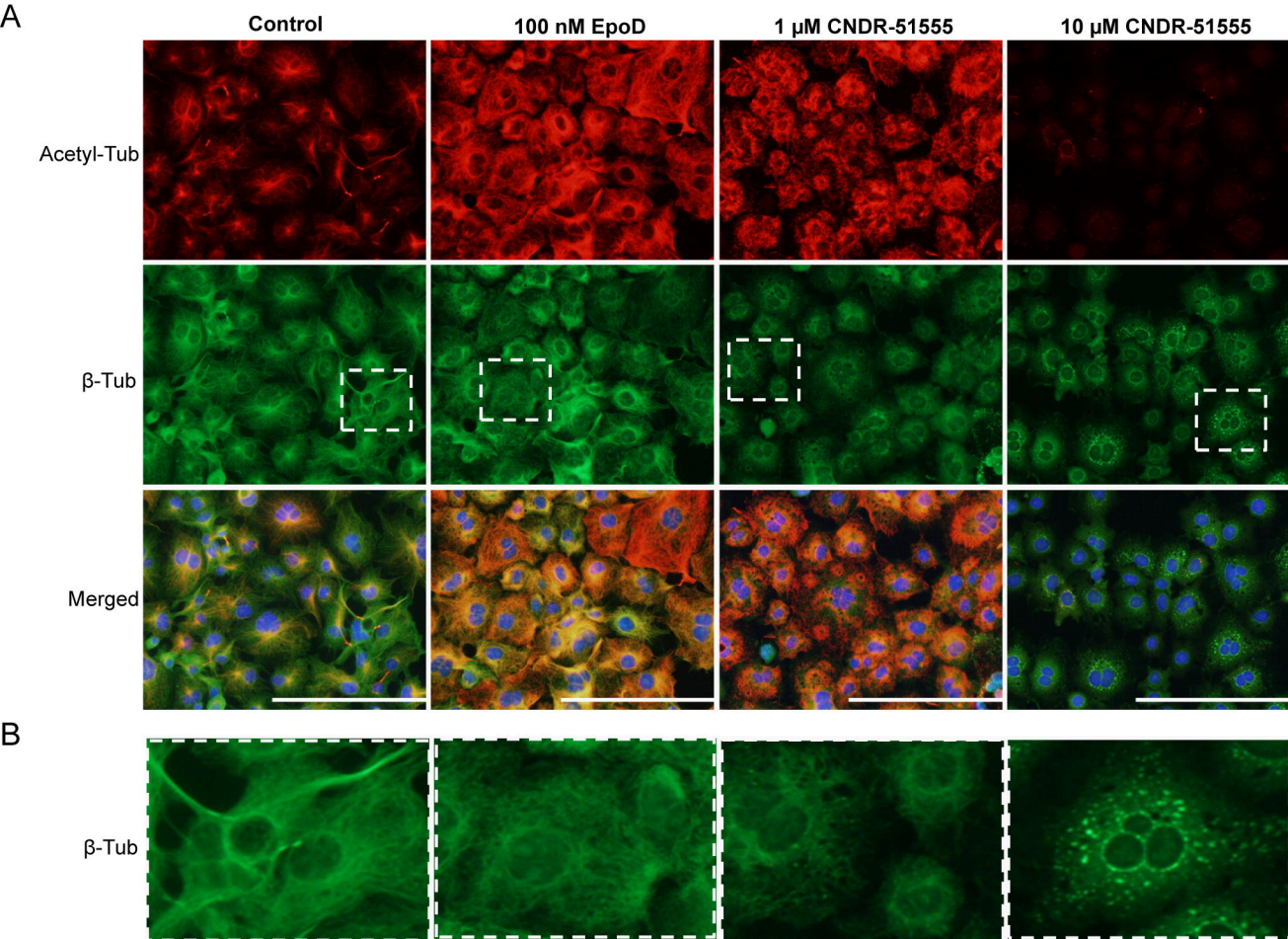


Figure 2.

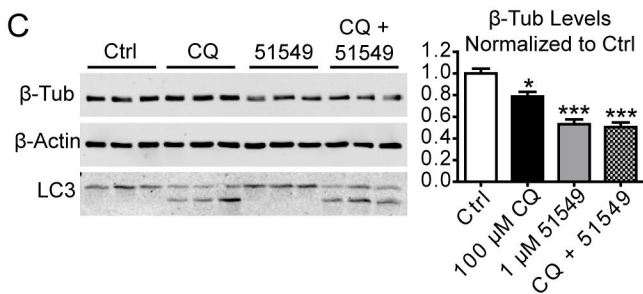
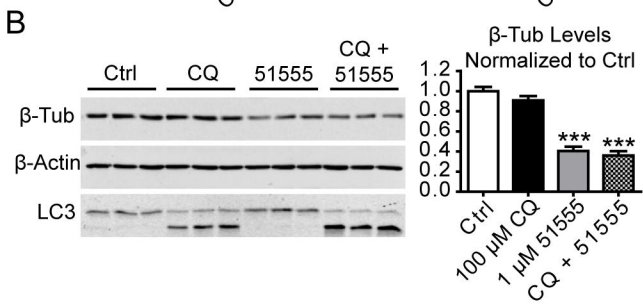
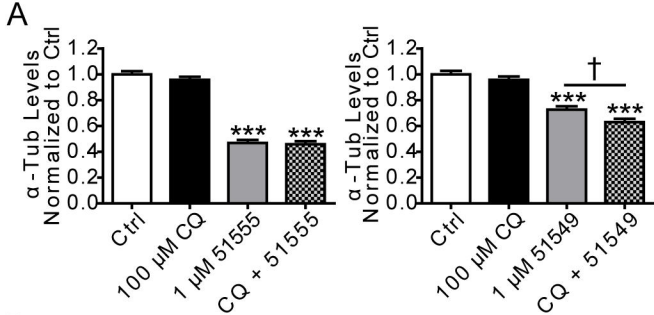


Figure 3.

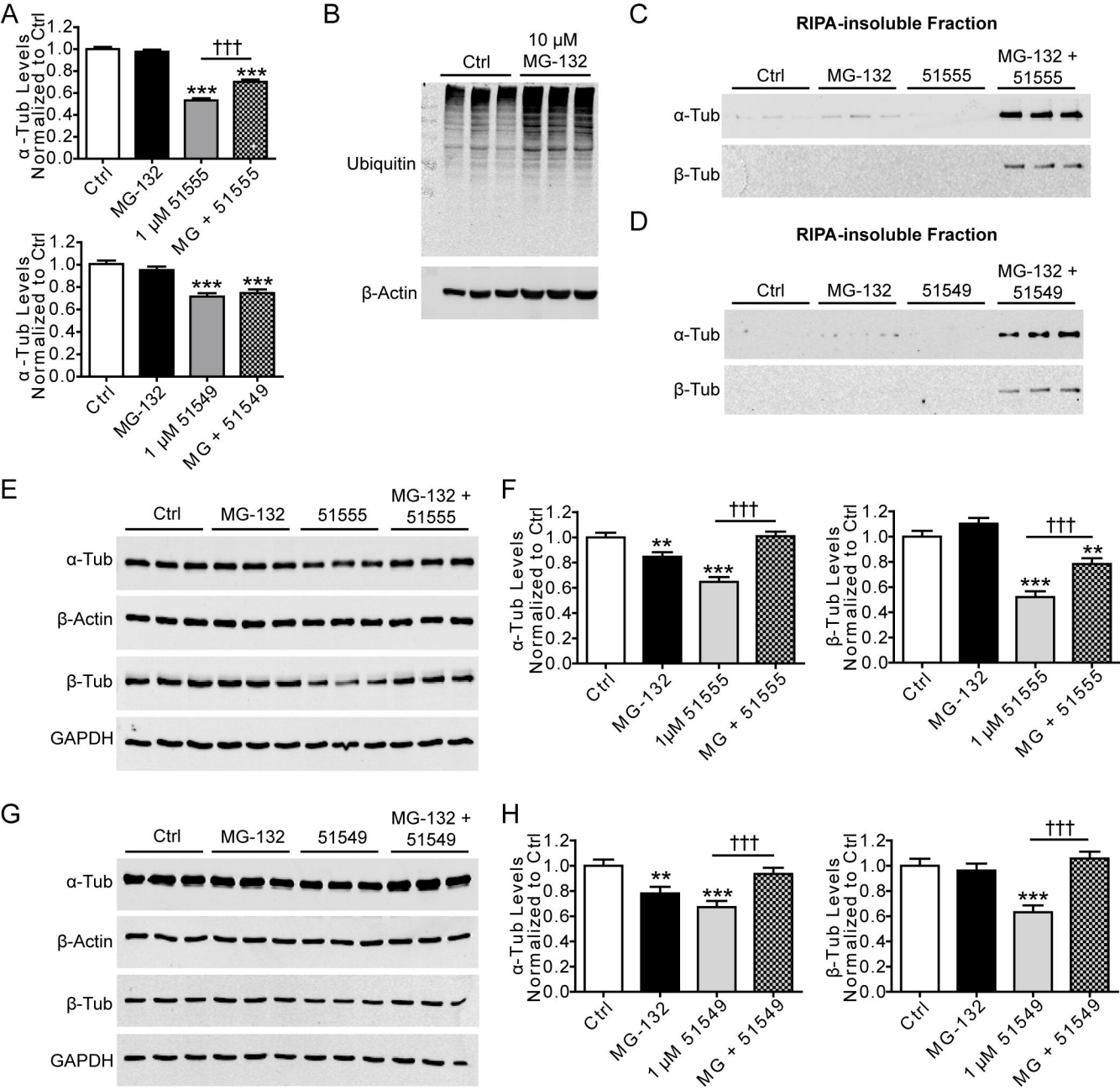


Figure 4.

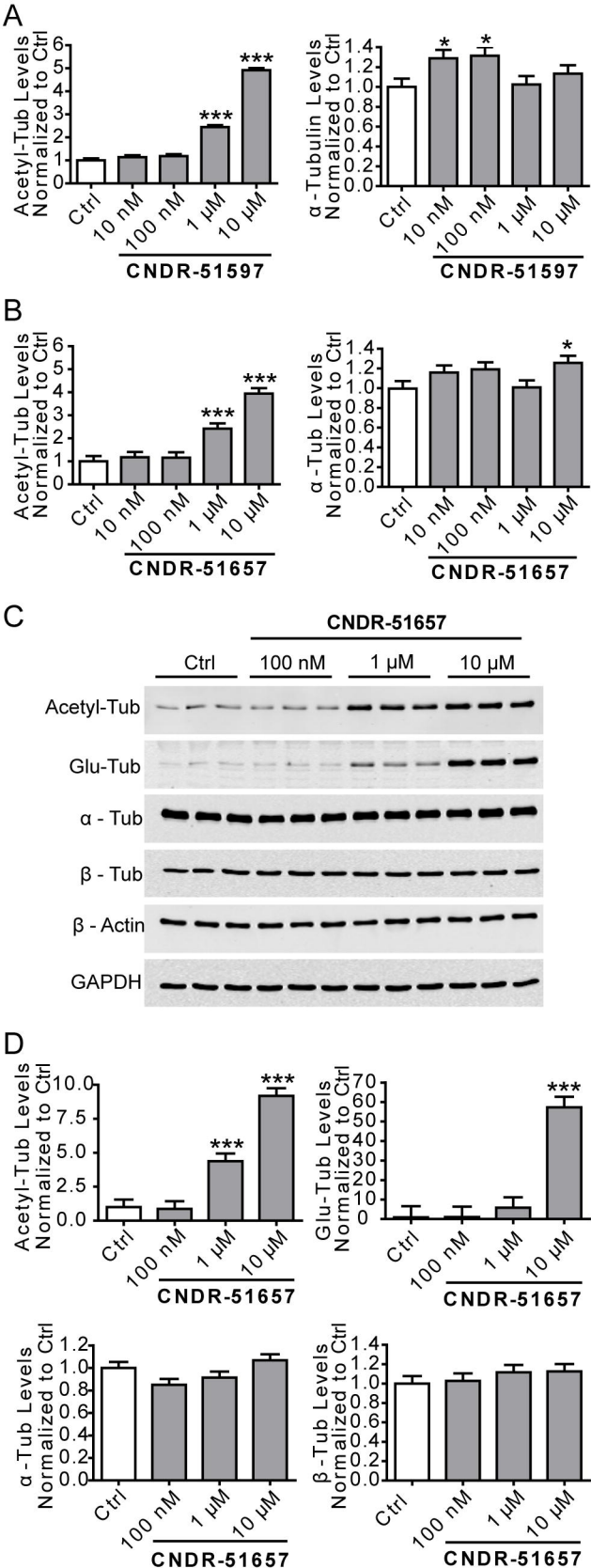


Figure 5.

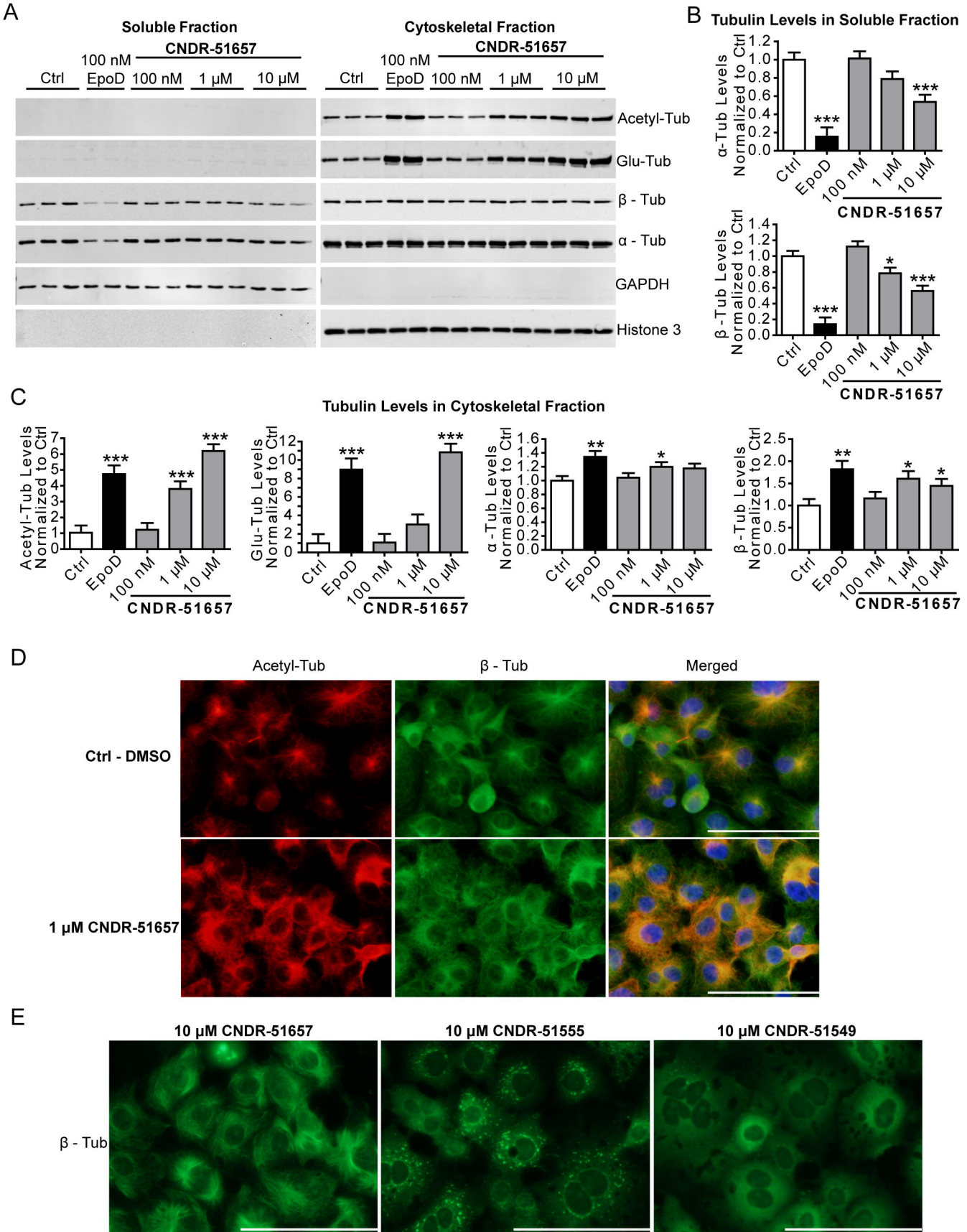


Figure 6.

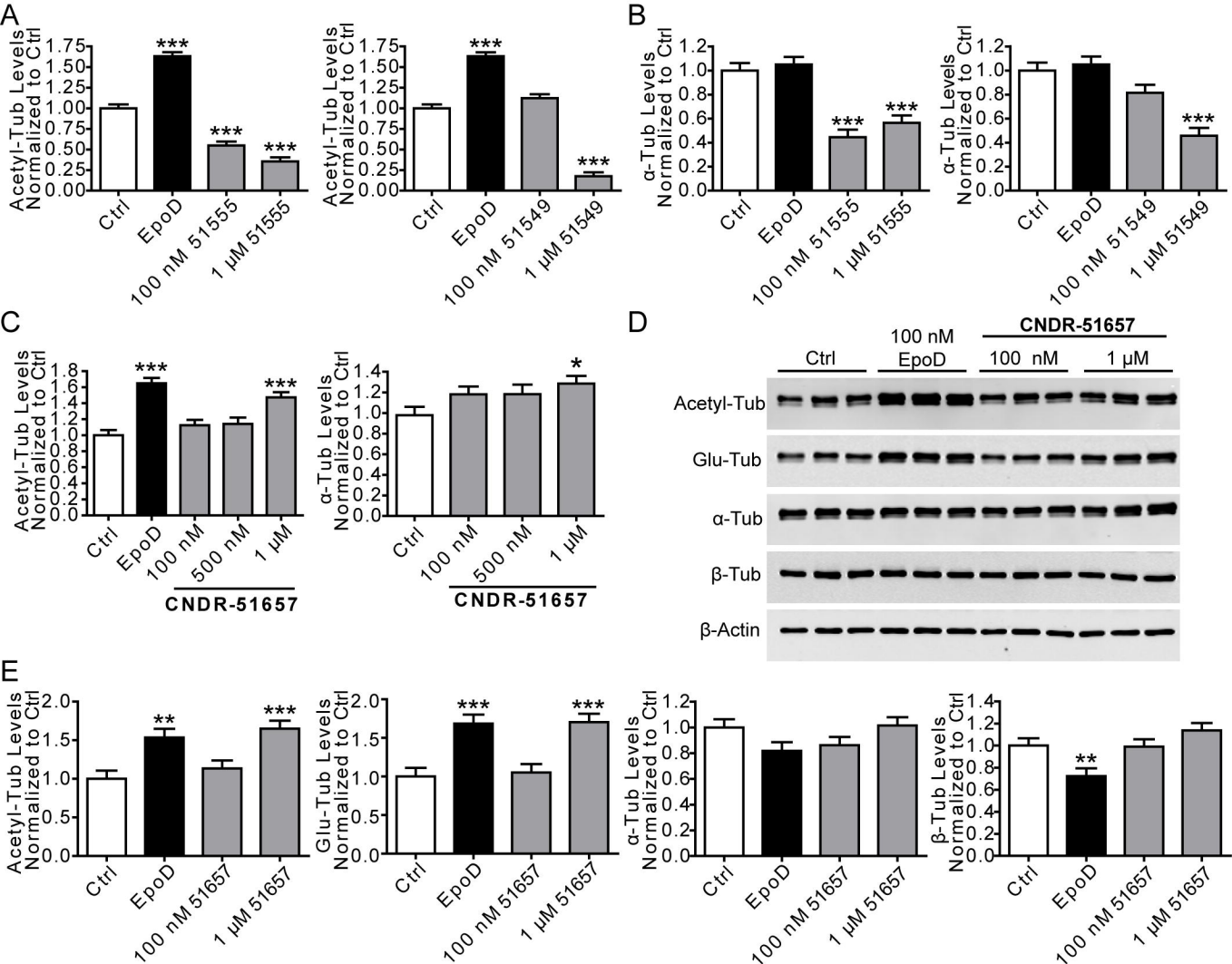


Figure 7.

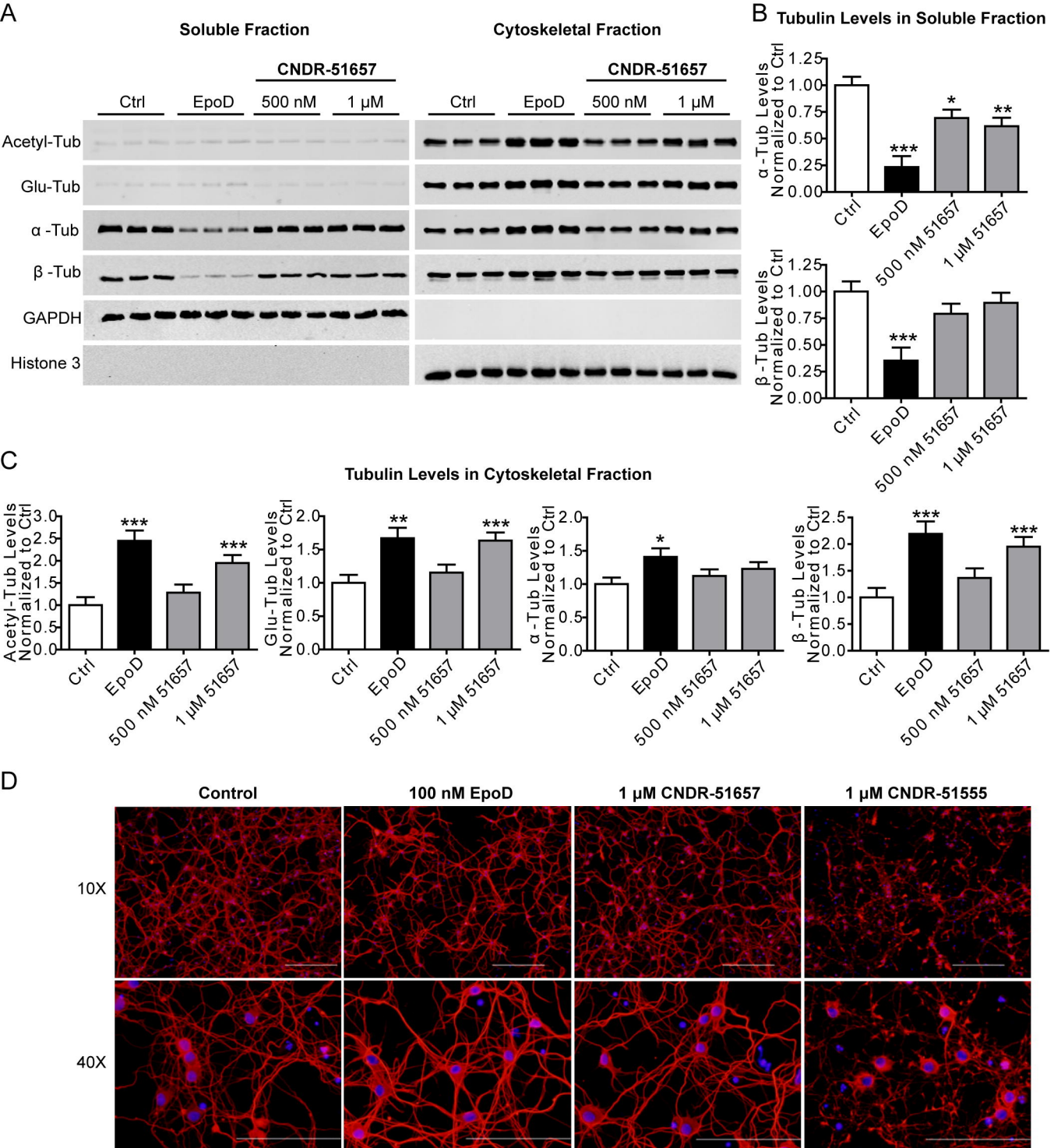
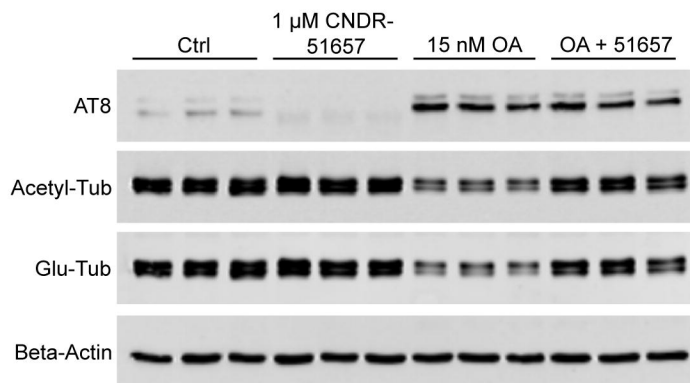
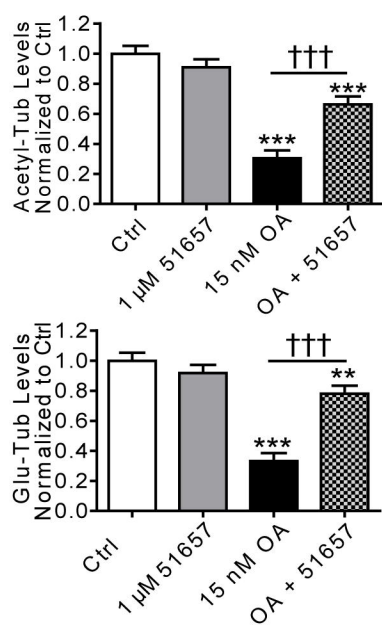


Figure 8.

A



B



C

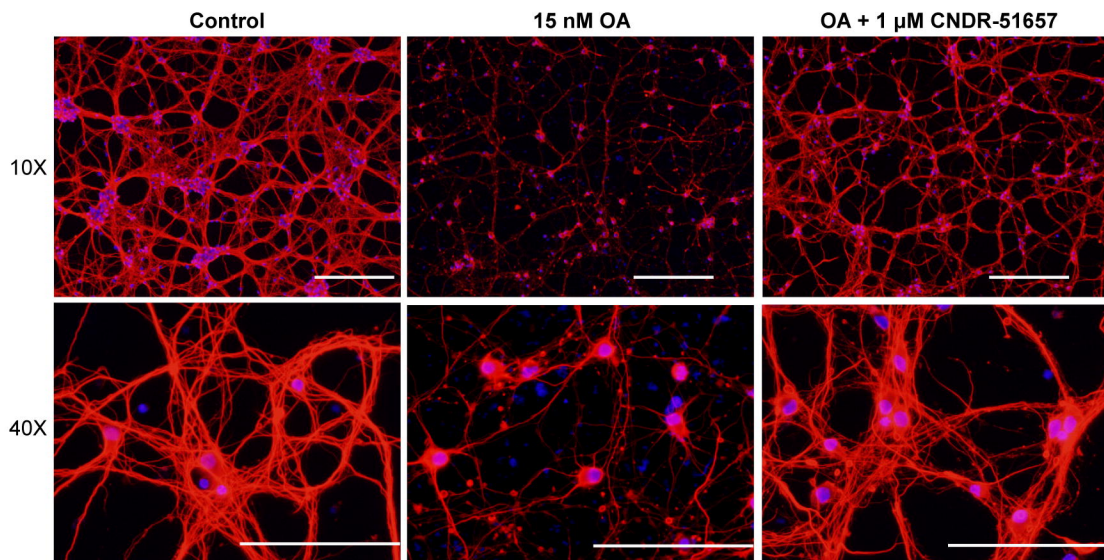


Figure 9.

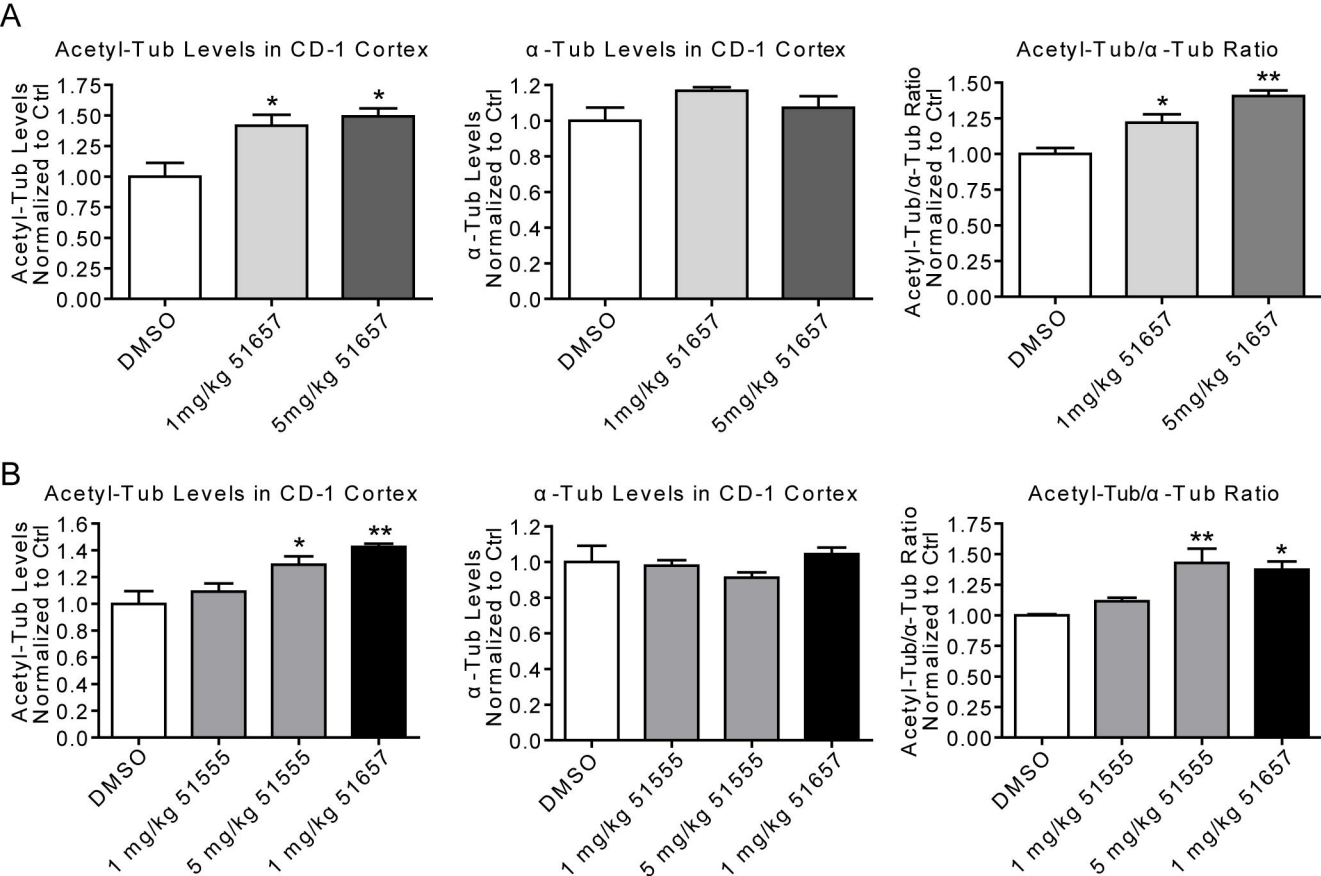


Figure 10.